A Middle to Late Miocene Trans-Andean Portal: Geologic Record in the Tatacoa Desert

C. Montes[1]*, C. A. Silva[2], G. A. Bayona[3], R. Villamil[4], E. Stiles[2,5], A. F. Rodriguez-Corcho[6], A. Beltran-Triviño[7], F. Lamus[1], M. D. Muñoz-Granados[4], L. C. Perez-Angel[8], N. Hoyos[1], S. Gomez[2,7], J. J. Galeano[1], E. Romero[7,2], M. Baquero[3], A. L. Cardenas-Rozo[7] and A. von Quadt[9]

[1]Universidad del Norte, Barranquilla, Colombia, [2]Center for Tropical Paleoecology and Archaeology, Smithsonian Tropical Research Institute, Ancón, Panamá, [3]Corporación Geologica Ares, Bogotá, Colombia, [4]Departamento de Geociencias, Universidad de Los Andes, Bogotá, Colombia, [5]Department of Biology, University of Washington, Seattle, WA, United States, [6]Schoool of Earth Sciences, University of Melbourne, Melbourne, VIC, Australia, [7]Departamento de Ciencias de la Tierra, Universidad EAFIT, Medellín, Colombia, [8]Department of Geological Sciences, Cooperative Institute for Research in Environmental Sciences (CIRES), Institute of Arctic and Alpine Research (INSTAAR), University of Colorado Boulder, Boulder, CO, United States, [9]Institute of Geochemistry and Petrology, Department of Earth Sciences, ETH Zurich, Zürich, Switzerland

Integration of several geologic lines of evidence reveals the prevalence of a lowland trans-Andean portal communicating western Amazonia and the westernmost Andes from at least middle Miocene until Pliocene times. Volcanism and crustal shortening built up relief in the southernmost Central and Eastern Cordilleras of Colombia, closing this lowland gap. Independent lines of evidence consist first, of field mapping in the Tatacoa Desert with a coverage area of ~381 km^2, 1,165 km of geological contact traces, 164 structural data points, and 3D aerial digital mapping models. This map documents the beginning of southward propagation of the southernmost tip of the Eastern Cordillera's west-verging, fold-and-thrust belt between ~12.2 and 13.7 Ma. Second, a compilation of new and published detrital zircon geochronology in middle Miocene strata of the Tatacoa Desert shows three distinctive age populations: middle Miocene, middle Eocene, and Jurassic; the first two sourced west of the Central Cordillera, the latter in the Magdalena Valley. Similar populations with the three distinctive peaks have now been recovered in western Amazonian middle Miocene strata. These observations, along with published molecular and fossil fish data, suggest that by Serravallian times (~13 Ma), the Northern Andes were separated from the Central Andes at ~3°N by a fluvial system that flowed into the Amazon Basin through the Tatacoa Desert. This paleogeographic configuration would be similar to a Western Andean, or Marañon Portal. Late Miocene flattening of the subducting Nazca slab caused the eastward migration of the Miocene volcanic arc, so that starting at ~4 Ma, large composite volcanoes were built up along the axis of today's Central Cordillera, closing this lowland Andean portal and altering the drainage patterns to resemble a modern configuration.

Keywords: Northern Andes, Andes, miocene, drainages, La Venta, portal, Magdalena valley

INTRODUCTION

Located between two major cordilleras in the Northern Andes (**Figure 1**), the Miocene deposits of the Tatacoa Desert, collectively known as "La Venta", have provided key insights into the paleogeography and the biodiversity of the Neogene in South America. La Ventan deposits contain the record of the Eastern Cordilleran uplift (Guerrero, 1993, Guerrero, 1997; Lundberg et al., 1998; Anderson et al., 2016), span a section of the Mid-Miocene Climatic Optimum—one of the most notable Cenozoic global warming events (Flower and Kennett, 1994; Zachos et al., 2001), and are the source of one of the best-studied Neotropical

terrestrial vertebrate assemblages in South America (Kay et al., 1997; Carrillo et al., 2015). The rich paleontological record of La Venta deposits has shed light on the evolution and biogeography of vertebrate lineages and the development of major drainage basins in South America. Arguably, one of the most relevant geological insights has been gained from fossil fish faunas preserved in La Ventan strata of the Tatacoa Desert. These fossils are evidence of a direct lowland connection between the Amazonian and the Magdalena drainage systems (i.e. an Andean portal) during middle Miocene times (Lundberg and Chernoff, 1992). This insight places tight constraints on the mode and timing of mountain growth, specially the presence
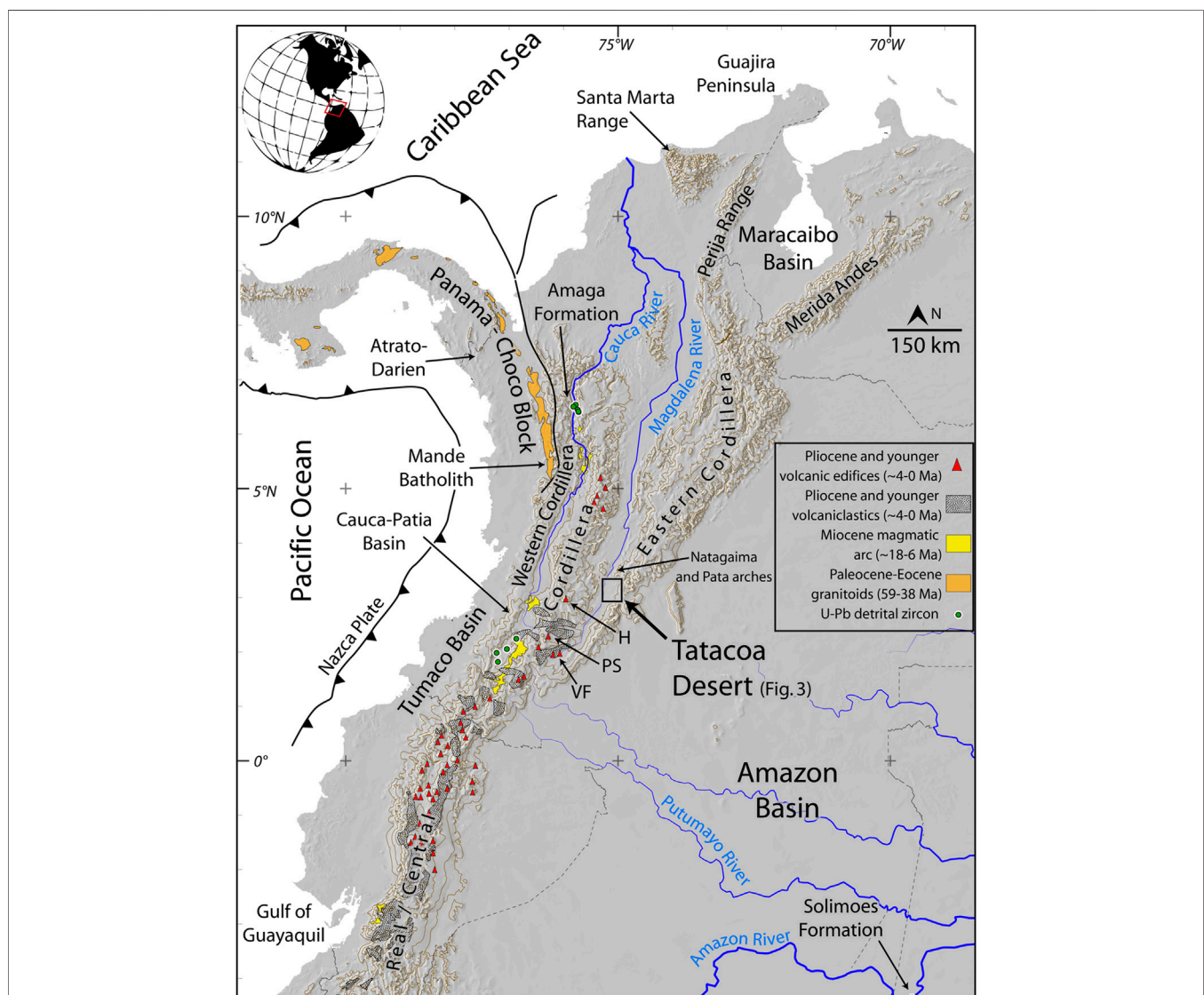
FIGURE 1 | General location map of the Northern Andes (the Andean block of Pennington, 1981), contour lines every 1,000 m. Green dots represent U-Pb detrital zircon samples: middle Miocene strata of the Amaga Formation (Montes et al., 2015), the Cauca-Patia Basin (Echeverri et al., 2015), and the Amazon Basin (Kern et al., 2020). The Miocene magmatic arc consists of hypabyssal porphyritic granitoids, while the Panama-Choco Eocene arc consists mostly of granitoids (Leal-Mejia, 2011; Montes et al., 2012; Bineli-Betsi et al., 2017; Leal-Mejia et al., 2019). Pliocene (~4 Ma) and younger ignimbrites and volcanoclastic rocks (Barberi et al., 1988; Torres-Hernandez, 2010; Egüez et al., 2017) represent the initial magmatic pulses in the construction of large composite active today in the Northern Andes (H: Huila Volcano, PS: Purace-Sotara volcanoes, VF: Villalobos-La Fragua volcanic center).
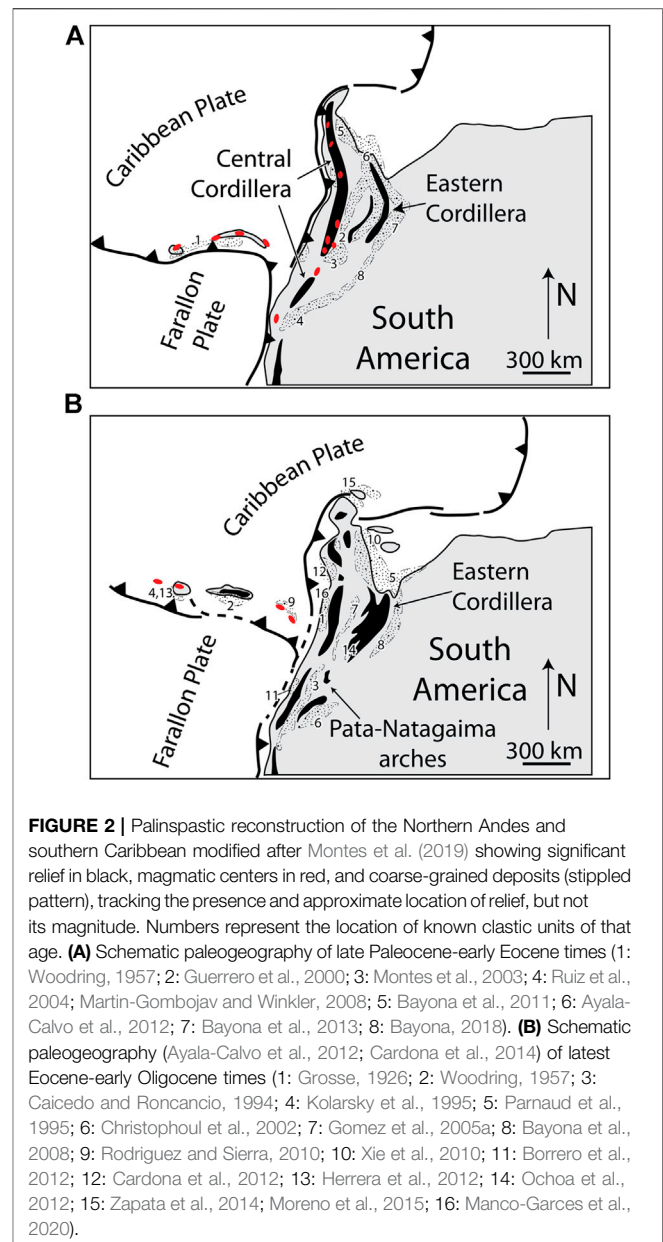
and timing of lowland portals that segmented the Andean cordillera of the past.

Equatorial lowland portals through the Andes have long been proposed to exist, variably called the Marañon, or Western Andean Portal (Hoorn et al., 1995; Lundberg et al., 1998; Antonelli et al., 2009; Hoorn et al., 2010). Such a lowland passage would have allowed equatorial (**Figure 1**) westward flow of major South American rivers (Hurtado et al., 2018), separating mountain-specific taxa between Central and Northern Andes (Antonelli et al., 2009), and joining lowland taxa of the Pacific and the Amazon (Haffer, 1967; Slade and Moritz, 1998; Miller et al., 2008; Weir and Price, 2011). Vanishing of such Late Cretaceous to middle Miocene times portal took place as a result of Andean topographic growth, as the raising orogen joined formerly isolated high Andean elevations, simultaneously segmenting formerly connected lowland drainage basins. There is however, little geologic data that more precisely pinpoint the location, and corroborate the presence of a lowland portal in the Northern Andes, and the time it remained opened.

In an attempt to better constrain Andean paleotopography, we focused our study on the gaps, or lowland portals that allowed the flow of major rivers across the Northern Andes. In this contribution we document the prevalence of low topography in a segment of the Northern Andes (~3°N) during Miocene times. By updating the geologic map of the Tatacoa Desert (Guerrero, 1993, Guerrero, 1997), and adding geochronological constraints to the existing stratigraphic framework (Flynn et al., 1997; Anderson et al., 2016), we established cartographic and geochronological criteria that helped trace the evolution of a major cross-Andean drainage. These new data, along with a compilation of existing data in the Northern Andes and Amazonia, bring into better focus the Miocene drainage networks and therefore, the timing and location of topographic growth in this part of the Northern Andes.

PALEOGEOGRAPHY OF THE TATACOA DESERT

Today, the Magdalena Valley is a large, longitudinal inter-Andean depression with variable widths between 20 and 40 km, whose evolution has been controlled by tectonic processes (Schamel, 1991; Van der Wiel and Van den Bergh, 1992) while maintaining a low topography of around 400 m a.s.l. (**Figure 1**). The Tatacoa Desert is located at the southern termination of the Magdalena Valley (**Figure 1**), loosely called a desert despite having precipitations of ~1,100 mm/yr and a dry forest cover (Hermelin, 2016). Its location in a leeward position with respect to the Eastern Cordillera, and bedrock geology characterize the Tatacoa Desert as badlands (Dill et al., 2020) with bedrock freshly exposed with no intervening regolith, extensive soil development or thick vegetation. It is in these badlands with nearly continuously exposed bedrock, long dip slopes, and frequent gullies, that the paleontological richness of La Venta strata has been abundantly documented within the stratigraphic framework defined by Guerrero (1993), Guerrero (1997).

FIGURE 2 | Palinspastic reconstruction of the Northern Andes and southern Caribbean modified after Montes et al. (2019) showing significant relief in black, magmatic centers in red, and coarse-grained deposits (stippled pattern), tracking the presence and approximate location of relief, but not its magnitude. Numbers represent the location of known clastic units of that age. **(A)** Schematic paleogeography of late Paleocene-early Eocene times (1: Woodring, 1957; 2: Guerrero et al., 2000; 3: Montes et al., 2003; 4: Ruiz et al., 2004; Martin-Gombojav and Winkler, 2008; 5: Bayona et al., 2011; 6: Ayala-Calvo et al., 2012; 7: Bayona et al., 2013; 8: Bayona, 2018). **(B)** Schematic paleogeography (Ayala-Calvo et al., 2012; Cardona et al., 2014) of latest Eocene-early Oligocene times (1: Grosse, 1926; 2: Woodring, 1957; 3: Caicedo and Roncancio, 1994; 4: Kolarsky et al., 1995; 5: Parnaud et al., 1995; 6: Christophoul et al., 2002; 7: Gomez et al., 2005a; 8: Bayona et al., 2008; 9: Rodriguez and Sierra, 2010; 10: Xie et al., 2010; 11: Borrero et al., 2012; 12: Cardona et al., 2012; 13: Herrera et al., 2012; 14: Ochoa et al., 2012; 15: Zapata et al., 2014; Moreno et al., 2015; 16: Manco-Garces et al., 2020).

In the following paragraphs, we review the landscape history of the southern Magdalena Valley in light of the Cretaceous and younger regional development of northwestern South America. The inception of a Cretaceous passive margin can be taken as a convenient starting point to review the history of landscape development in the Northern Andes. Regionally continuous Cretaceous strata document the persistence of a west-facing oceanic margin (Etayo-Serna, 1994; Moreno-Sanchez and Pardo-Trujillo, 2003), with source areas located to the east, in the Guiana shield (Villamil, 1998; Horton, 2018; Sarmiento-Rojas, 2018).
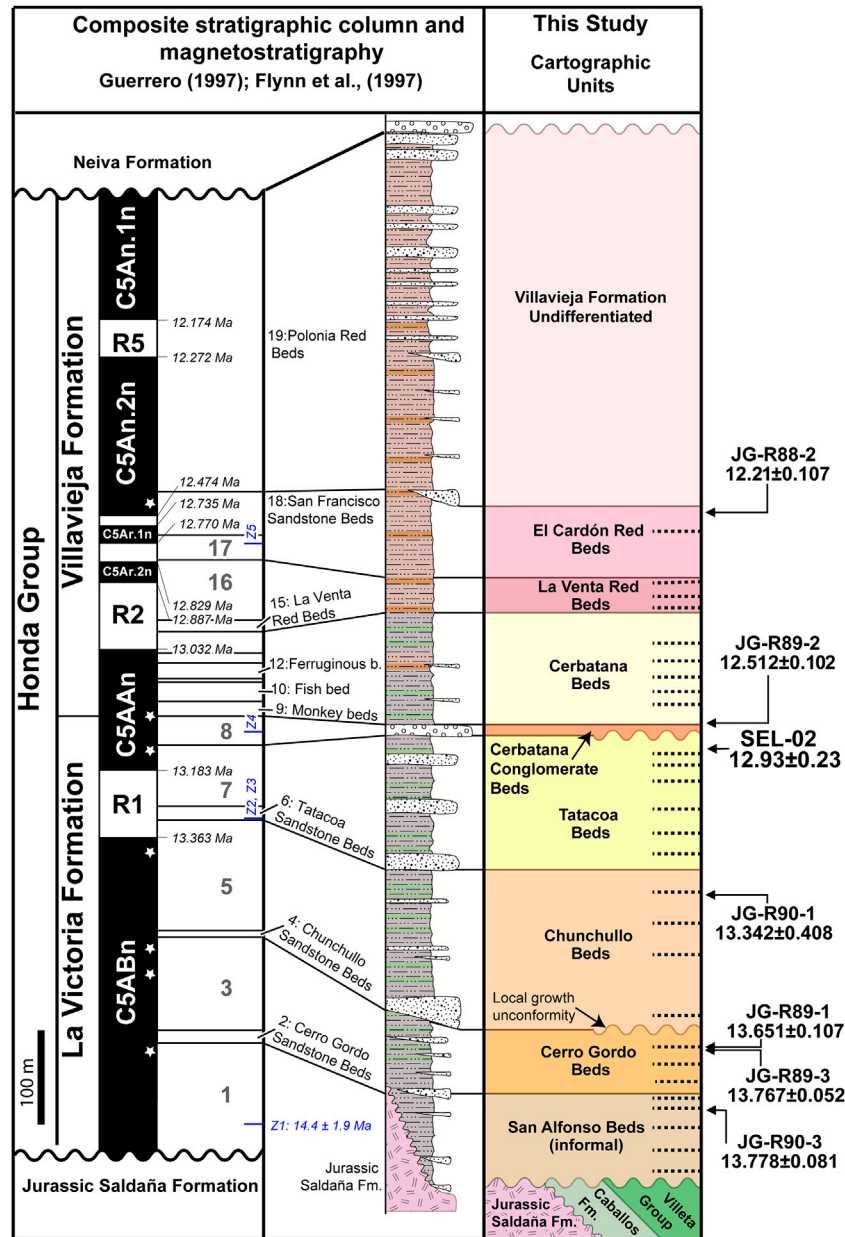
FIGURE 3 | Updated stratigraphic scheme for the Honda Group in the Tatacoa Desert. The original columns of Guerrero (1993, 1997), were consolidated into a single composite column where lenticular beds represent discontinuous sandstone units (i.e. found in only one stratigraphic column), and mudstones according to their color (Anderson et al., 2016). Magnetostratigraphy covers the C5An.1n-C5ABn interval, showing updated ages after Hilgen et al. (2012). Black arrows represent geochronological samples from Flynn et al. (1997), blue arrows represent maximum depositional ages of Anderson et al., (2016). All samples were re-located (stars) in the stratigraphic column following the lithostratigraphic marker beds (horizontal dashed lines) of the geologic map (**Figure 4**).

Latest Cretaceous-Early Eocene

Collision of oceanic terranes against the Cretaceous passive margin of northwestern South America marked the start of a regional marine regression, and gradual installation of swampy environments where locally thick coal beds were deposited (Bayona et al., 2011). These swamps were bound to the west by a primordial, probably discontinuous, eastwardly-tilted Central/Real Cordillera (**Figure 2A**), and to the east by isolated intra-plate uplifts (Villamil, 1999; Gomez et al., 2003; Gomez et al., 2005b; Bayona et al., 2011; Bayona et al., 2020). This tectonically-forced marine regression may have started as early as latest Cretaceous to the south in the Oriente Basin, reaching the northern end of the orogen in the Guajira region in middle Paleocene times, taking ~10 million years to propagate from south to north (Jaimes and de Freitas, 2006; Martin-Gombojav and Winkler, 2008; Weber et al.,

2009a; Weber et al., 2009b; Bayona et al., 2011; Cardona et al., 2011; Hurtado et al., 2018). Upper Cretaceous coarse-grained clastic deposits track the location of this orogen to segments of today's Central Cordillera (Schamel, 1991; Montes et al., 2019), a mountain range that would have constricted most westward-directed drainages in northern South America, spawning the first north- or northeastward-directed Orinoco style drainages (Hoorn et al., 1995; Lundberg et al., 1998; Hoorn et al., 2010; Bande et al., 2012; Horton, 2018; Hurtado et al., 2018).

Middle Eocene-Oligocene

In middle Eocene to Oligocene times, contractional deformation concentrated along the eastern foothills of the Central Cordillera, or internal uplifts in the Magdalena Valley, where conglomerate units (Tesalia/Chicoral, in the south, and La Paz formations in the north) unconformably accumulated upon Cretaceous and Jurassic sequences (Ramon and Rosero, 2006). By late Eocene times contractional deformation propagates eastward, to the domains of the Eastern Cordillera where westward-verging, north-trending thrust faults started defining a north-south, en-echelon fold belt that defines a young—yet incomplete—Magdalena Valley north of ~4°N (Reyes-Harker et al., 2015). The Magdalena Valley would have been defined by a topographic depression between two flanking, linear, probably discontinuous mountain ranges (**Figure 2B**): a primordial Central Cordillera to the west (Gomez et al., 2003; Gomez et al., 2005a; Nie et al., 2010; Nie et al., 2012; Horton et al., 2015) and the young Eastern Cordillera to the east (Mora et al., 2006; Bande et al., 2012; Bayona et al., 2013; Lamus et al., 2013). South of ~4°N, near the latitude of the Tatacoa Desert, the mountainous highland terrain of the Eastern Cordillera would have gently eased into the lowlands of the Amazon/Orinoco (Mora et al., 2013), only interrupted by isolated intra-basin uplifts.

In the area centered around the Tatacoa Desert, the entire 2.3 km thick, Cretaceous-Paleocene regional succession of the southern Magdalena Valley (Amezquita and Montes, 1994), is missing (see Figure 5B in Caballero et al., 2013). The Lower to Middle Jurassic volcanic, volcanoclastic mechanical basement of the Saldaña Formation (Cediel et al., 1980; Mojica and Franco, 1990) is covered by the middle Miocene strata of the Honda Group in a marked angular unconformity. This unconformity has been variably mapped as the arch of Natagaima, or Pata (**Figure 1**), resulting from a period of deformation, exhumation and erosion that removed the passive margin succession sometime between Eocene and early Miocene times (Schamel, 1991; Amezquita and Montes, 1994; Villarroel et al., 1996; Ramon and Rosero, 2006), correlative to the middle Eocene unconformity to the north in the middle Magdalena Valley (Gomez et al., 2005b). The Jurassic basement of the Natagaima Arch indeed records cooling peaks at 30 and 50 Ma (apatite fission-track in Saltaren-1 well, Reyes-Harker et al., 2015), consistent with exhumation and erosion removing most of the Cretaceous strata in the area now occupied by the Tatacoa Desert.

Miocene

By middle Miocene times the area formerly undergoing exhumation and erosion in the arches of Natagaima and Pata began subsiding, opening accommodation space to accumulate fluvial strata of the ~1,000 m thick Honda Group (Guerrero, 1993, 1997).

### Stratigraphy of the Honda Group

In general terms, the Honda Group is a monotonous stratigraphic unit dominated by fining-upward, gray lithic sandstone beds (**Figure 3**), that can be easily recognized all along the southern Magdalena Valley between the ~2° and ~5°N latitude, but never in the surrounding Eastern and Central Cordilleras. Large faults of the bounding cordilleras thrust crystalline basement on to strata of the Honda Group, deforming it, and making it the youngest significantly deformed strata in the southern Magdalena Valley (Van der Hammen, 1958). West-verging, low-angle crystalline thrust sheets of the Eastern Cordillera place the Jurassic volcanoclastic Saldaña Formation (~3°N, Prado Fault, Cossio et al., 1995), and metamorphic rocks of the Garzon Massif (~2°N, Iskana-1 well, Saeid et al., 2017), on top of strata of the Honda Group. East-verging, low-angle thrust faults place Jurassic intrusives on top of strata of the Honda Group along the eastern flank of the Central Cordillera (~3°N, Amezquita and Montes, 1994).

The base of the Honda Group is marked by either an angular unconformity atop Jurassic-Cretaceous strata, or a paraconformity on strata of the Oligocene Gualanday Group, or La Cira Formation (Van der Hammen, 1958; Guerrero, 1997). The upper Miocene/Pliocene Neiva/Gigante formations rest in angular unconformity atop strata of the Honda Group (Van der Hammen, 1958; Guerrero, 1997) in the south of the Magdalena Valley (~2°N), or the Pliocene Mesa Formation to the north (~5°N).

From bottom to top the Honda Group was divided by Guerrero (1993, 1997) into two units: the La Victoria Formation, and the Villavieja Formation. The same author discriminated nineteen different horizons within the ~1,000 m thick sequence (**Figure 3**), mapping seven of them throughout parts of the Tatacoa Desert (**Figure 4**), and giving informal names of important paleontological localities to three of them: the Monkey, Fish, and Ferruginous beds (**Figure 3**). Within the La Victoria Formation, Guerrero (1993, 1997) recognized four conspicuous horizons, from bottom to top: the Cerro Gordo, Chunchullo, Tatacoa, and Cerbatana, the first three made up by sandstone beds and bedsets, and the last one a conglomerate bed, also marking the top of the La Victoria Formation. The intervening stratigraphic horizons were left unnamed.

Age of the Honda Group

The age of the Honda Group in the Tatacoa Desert was tightly constrained using magneto-stratigraphy (intervals C5An.1n - C5ABn of Cande and Kent, 1992) tied to six Ar/Ar ages in plagioclase and hornblende crystals from pumice fragments within eight "volcanic units" (Flynn et al., 1997). Although no truly volcanic ash beds were identified in strata of the Honda Group, the upsection decrease in youngest detrital zircon ages
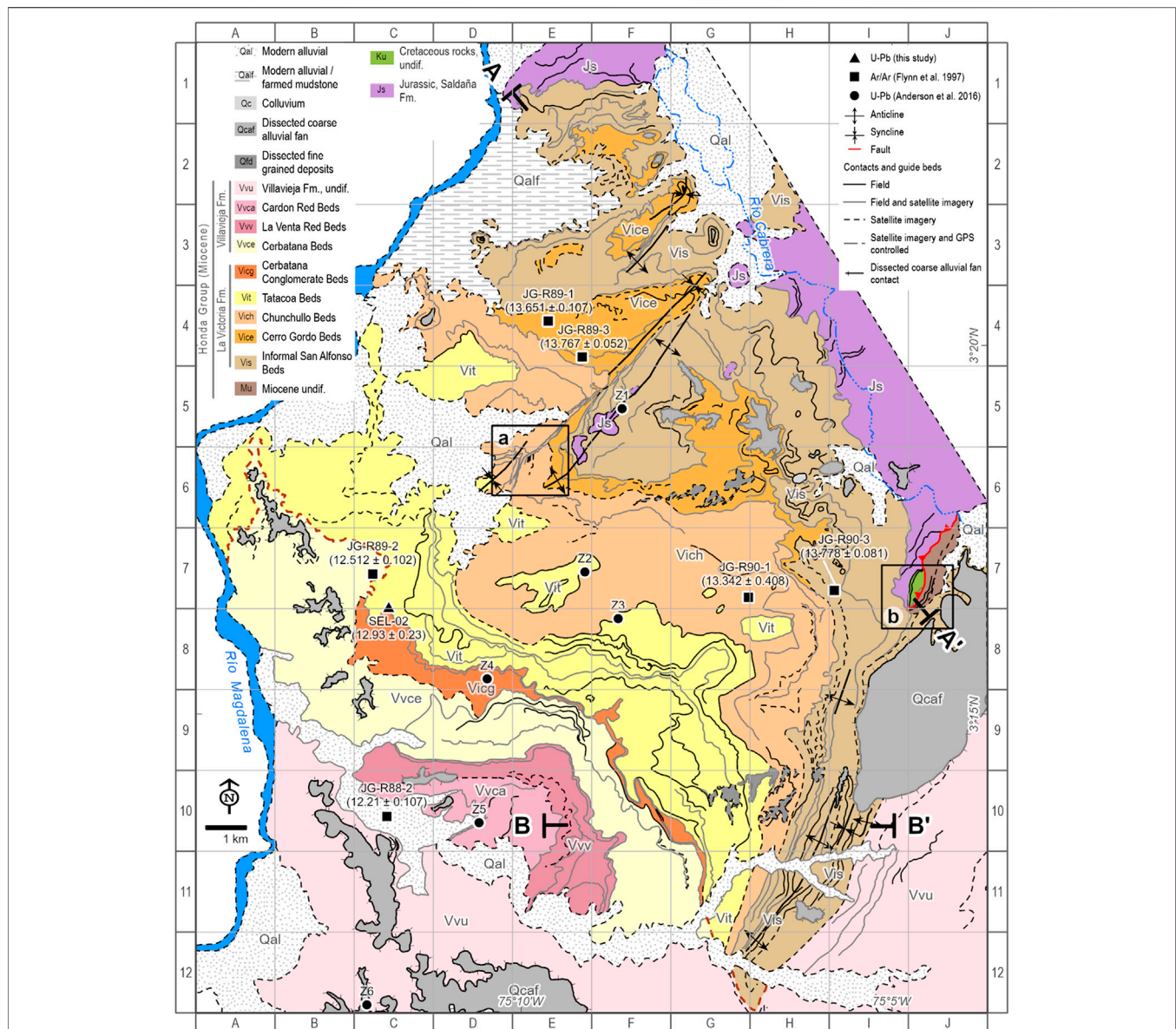
FIGURE 4 | Geologic map of the Tatacoa Desert expanded from original mapping by Guerrero (1993, 1997). The Tataoca Desert is bound to the west by the Magdalena River, to the east by the first ranges of the Eastern Cordillera, to the north by the volcaniclastic outcrops of the Jurassic Saldaña Formation in the Natagaima Arch, and to the south by strata of the overlying Neiva Formation. A larger-scale, printable at 1:25.000 version available of the map also available (Supplementary Figure S1), as well as an electronic .kml version with contacts and data stations in the Supplementary Materials.

was taken as evidence of syndepositional volcanism within the drainage basin (Anderson et al., 2016). Pumice fragments within volcanoclastic sandstones of the Honda Group show evidence of reworking since the time of eruption, but the lag time between eruption and sediment deposition was considered to be short, so Ar/Ar ages were used as near-depositional ages, and as tie points for magneto-stratigraphic reversal matching assuming no major hiatuses within the sequence (210 samples, yielding an interval between 11.6 and 13.5 Ma, Flynn et al., 1997). Despite updates to the chronology of intervals C5An.1n

- C5ABn (Hilgen et al., 2012), the correlation of the magnetic polarity stratigraphy of the Honda Group of Flynn et al. (1997) remains unchanged (**Figure 3**). More recent U-Pb detrital zircon geochronology suggests an earlier start for the accumulation of the Honda Group (14.4 ±1.9 Ma) using the cluster of youngest detrital zircon grains from five samples of Honda Group sandstone in the Tatacoa Desert (samples Z1 to Z5 of Anderson et al., 2016).

Fluvial strata within the lower Villavieja Formation contain fossil fish with Amazonian affinities like the giant Pirarucu,

Arapaima gigas, and many others riverine fish. These findings imply that at the time of deposition of these strata, large meandering river systems (Guerrero, 1997) were connected to the Amazonian drainage system (i.e., no continuous southernmost Eastern Cordillera, Lundberg and Chernoff, 1992; Albert et al., 2006; Ballen and Moreno-Bernal, 2019). This connection would have been severed by topographic growth of the Eastern Cordillera as west-verging structures (Schamel, 1991; Saeid et al., 2017) built topography after accumulation of strata of the Honda Group, and seem to have definitely established the Eastern Cordillera south of 4°N.

In summary, the area now occupied by the Tatacoa Desert preserves a record of most episodes in the growth and evolution of the Northern Andes. First, it contains the record of a stable Late Cretaceous passive margin in an embayment open to the north. Then, deformation, exhumation and erosion formed an isolated intrabasin uplift in Eocene-Oligocene times. Later in Miocene times, subsidence formed a sub-Andean sedimentary basin open to the lowlands of the Amazon to the east. This Miocene basin contains the record of the last lowland hydrologic connection between the Caribbean and the Amazon before forming the fully inter-Andean valley of today.

METHODOLOGY

Field Mapping

Traditional geologic mapping was performed at 1:25.000 scale using Brunton compass, colored pencils, and paper maps (IGAC topo sheets: 303-III-A and C, 303-I-C, 302-IV-B and D, and 302-II-D). Because the low dips, monotonous sequence, and nearly complete absence of conspicuous marker beds, it is often difficult to establish the stratigraphic position of individual beds within the Miocene sequence of the Tatacoa Desert. Additionally, local relief in the Tatacoa Desert is subtle, with changes in elevation along field transects rarely exceeding 50 m. Field mapping was focused on deciphering superposition relations amongst beds and bed sets by following prominent cliff-forming strata along-strike for several kilometers. These cliffs, often less than 20 m high, are defined by sandstone or conglomerate beds more resistant to erosion, while gentler topography represents massive mudstone. By repeating this exercise in multiple transects, it was possible to construct a framework of superposed cliff-forming beds, and bed sets that allows lateral lithostratigraphic correlation to the stratigraphic succession of units defined by Guerrero (1993, 1997). In the northern third of the mapping area, topography is more subdued, dips are lower, with less prominent sandstone beds, so the approach described above was combined with a systematic collection of control points using hand-held GPS units.

Once the field map was completed, the contacts were digitized in QGIS and their location accuracy was checked using Google Earth satellite imagery (2013 and newer imagery). All contacts, control points and dip data are contained in .kml files (see Supplementary Material). Each geologic contact contains an attribute that indicates its origin, and the nature of post-processing, if any. Contacts mapped in the field, with no changes made during post-processing have the attribute "*Obs.field*"; contacts adjusted during post-processing are coded as "*Obs.field+i*". New contacts added during post-processing are identified as "*imagery*" and usually needed to map alluvial deposits, or extend beds mapped in the field. Contacts needed to topologically close polygons were labeled as "*border*".

We measured dip data on sandy beds, avoiding cross beds, channelized beds and clinoforms. Although it would have been preferable to measure dip data on fine-grained sediments, the massive nature, and poorer exposure of most mudstone sections prevented a systematic collection of dip data in these lithologic types. Whenever possible, we averaged out local irregularities on sandstone tops by selecting a view of a planar bedding surface, moving laterally until the two-dimensional surface appeared as a line, taking a level sight to the trace of the planar surface, and then the strike of the same sight line, later converted to dip direction (Compton, 1985).

We used oblique ortho-photos to document changing dip domains in selected, low relief, key areas of the Tatacoa Desert. We collected 338 vertical photographs at 60 m-altitude to generate a detailed 3D model of 7.83 Ha using Agisoft Metashape software. We then converted a 131-million-point cloud into a 2.8-million faces mesh with photographic texture. In order to detect beds in the 2.74 cm/pix 3D image, we employed the original 1.37 cm/pix image resolution using a textured tiled model. We used OpenPlot (Tavani et al., 2011) in 101 triangles joining single bed points to measure attitudes.

Detrital Zircon U-Pb Geochronology

Detrital zircon separation was performed at EAFIT University facilities following standard procedures such as those proposed by Mange and Maurer (1991). Rock samples were crushed in a conventional jaw-breaker and sieved various fractions. Heavy minerals were concentrated by panning the 400–63 µm fraction. Zircon grains were randomly picked-out by hand using a binocular lens from the heavy mineral concentrates, mounted in epoxy resin and polished down to be coated by carbon at ETH Zurich. Cathodoluminescence (CL) images of zircon grains were acquired to evaluate magmatic zoning, metamorphic origin or inherited cores in a Vega 3 scanning electron microscope (SEM) at the scientific center for optical and electron microscopy (ScopeM) at ETH Zurich. *In situ* U-Pb geochronology were conducted by laser ablation inductively coupled plasma mass spectrometry (LA-ICP-MS) at the Institute of Geochemistry and Petrology at ETH Zurich using a 193 nm Resolution (S155) ArF excimer laser coupled to a Element SF ICPMS (Guillong et al., 2014; Von Quadt et al., 2014). Laser ablation spots (19 microns) were selected in both cores and rims when it was possible. The full analytical dataset is reported in Table SM-1. Age uncertainties (at 2σ) for individual grains in the data table include only measurement errors. Interpreted ages are based on $^{206}Pb/^{238}U$ for grains younger than 800 Ma and $^{206}Pb/^{207}Pb$ for grains older than 800 Ma. Analyses that were >30% discordant (by comparison of $^{206}Pb/^{238}U$ and $^{206}Pb/^{207}Pb$ ages), or >5% reverse discordant, or >4% error age were not considered

FIGURE 5 | Field photographs of strata of the Honda Group. **(A)** Trough cross-stratified (arrows) medium-grained sandstone with imbricated pebbles of the Cerbatana Conglomerate Beds (quadrangle G11 in **Figure 4**). **(B)** Mudstone at the base of the San Alfonso Beds, near Cerro Gordo (quadrangle F5 in **Figure 4**). **(C)**, **(D)** Mud-cracks and erosive contact respectively, in red muddy/sandy strata of the San Alfonso Beds (quadrangle H10 in **Figure 4**). **(E)** Sharp basal contact (arrow) of the Cerbatana Conglomerate Beds (quadrangle D8 in **Figure 4**). **(F)** Gently dipping strata in the Chunchullo Beds in quadrangle H9 in **Figure 4**, notice the mappable sandstone beds and bed sets within the sequence (arrows). **(G)** Dissected alluvial deposits (black arrow) capping strata of the Cerro Gordo Beds marked by white arrow (quadrangle G5 in **Figure 4**). Inset shows close up of alluvial deposits showing the typical size distribution.
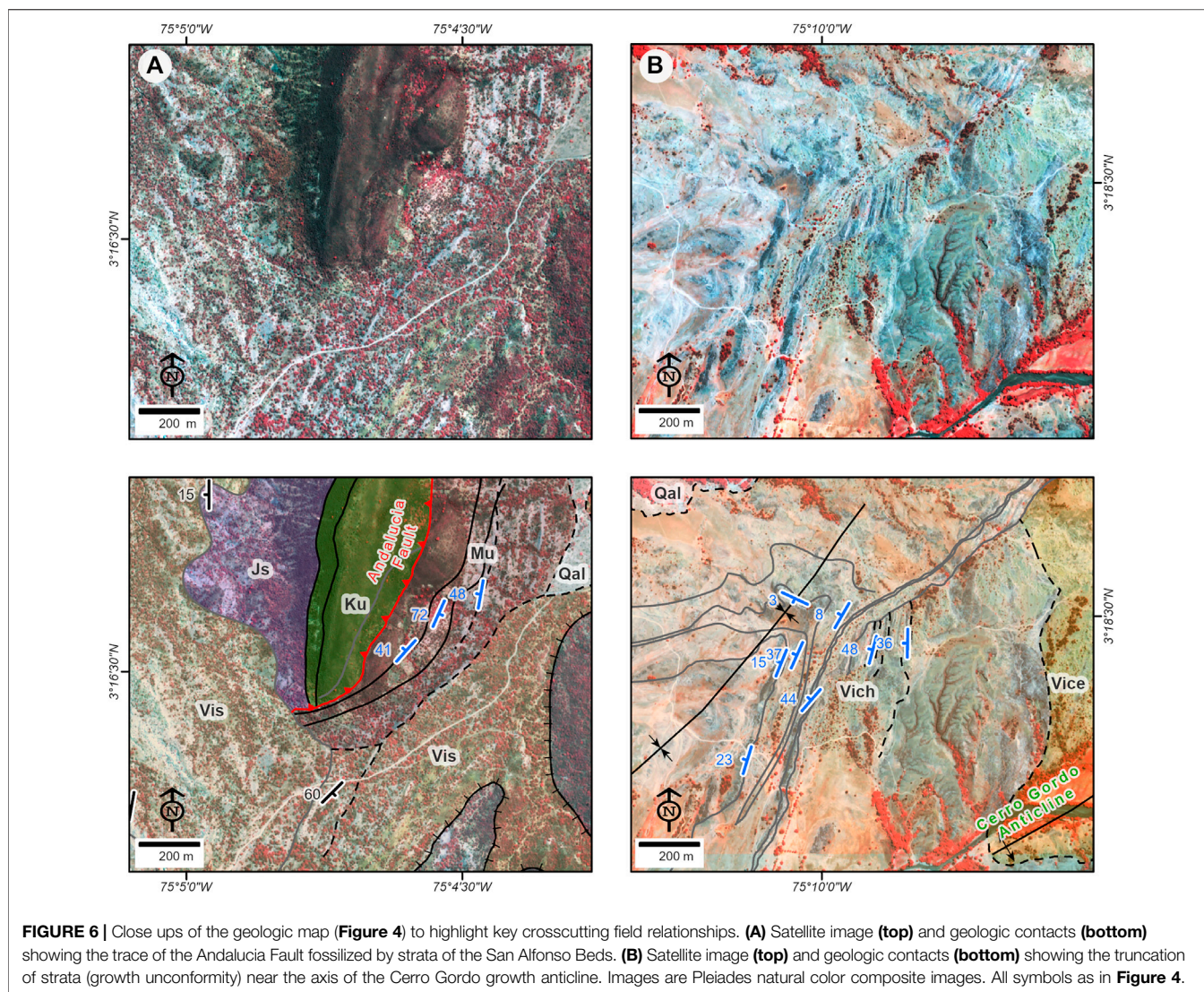
further. Uranium-Pb Concordia diagrams are constructed using Isoplot4.15 (Ludwig, 2012). We show the Tera and Wassergburg (1972) concordia diagram (^{238}U/^{206}Pb - ^{207}Pb/^{206}Pb) to focus on Mesozoic and Cenozoic zircon ages.

We calculated detrital zircon MDA (maximum depositional age) using the method of the weighted average of the youngest concordant three zircons (Y3Z), in our case, the date overlaps within 2σ uncertainty. An assessment of detrital zircon MDA estimation methods (Coutts et al., 2019) suggests that the Y3Z method is more successful and accurate than other methods such as the young grain cluster at 2σ uncertainty (YGC 2σ; Dickinson and Gehrels, 2009). The weighted average MDA was calculated by using the algorithm in Isoplot 4.15 (Ludwig, 2012).
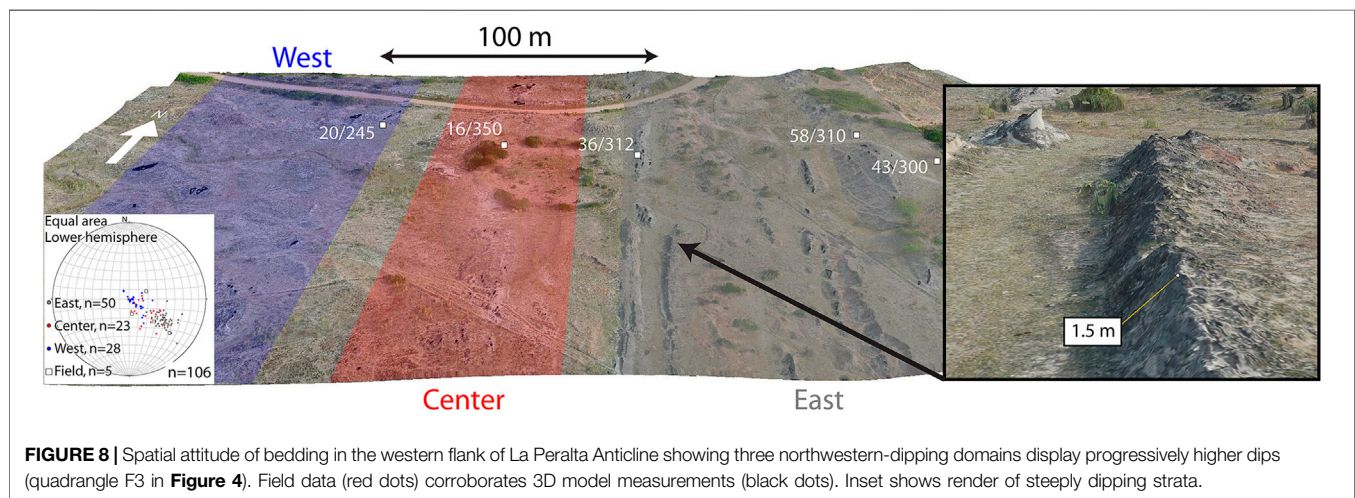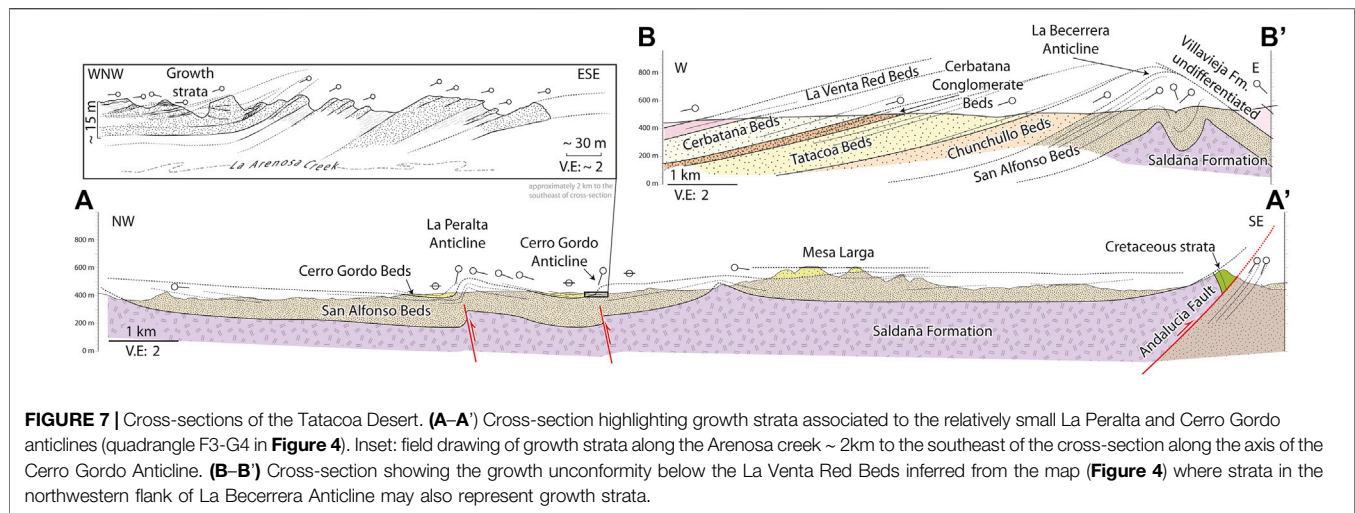
RESULTS

Geologic Map

The updated geologic map of the Tatacoa Desert covers an area of 381 km^2, contains 1,165 km of contact traces, and 164 structural control points. This map (**Figure 4**) broadens the distribution of strata within the La Victoria and Villavieja formations of Guerrero (1993, 1997) to the entire extent of the Tatacoa Desert. We keep existing stratigraphic and structural nomenclature, using the name of the seven most prominent (**Figure 3**) sets of beds identified in Guerrero's map (1993, 1997). Our map documents the presence of two growth unconformities within the Honda Group discussed in the following paragraphs.

FIGURE 6 | Close ups of the geologic map (**Figure 4**) to highlight key crosscutting field relationships. (**A**) Satellite image (**top**) and geologic contacts (**bottom**) showing the trace of the Andalucia Fault fossilized by strata of the San Alfonso Beds. (**B**) Satellite image (**top**) and geologic contacts (**bottom**) showing the truncation of strata (growth unconformity) near the axis of the Cerro Gordo growth anticline. Images are Pleiades natural color composite images. All symbols as in **Figure 4**.

Being a characteristically fining-upwards unit, we decided to use each one of the horizons defined and mapped by Guerrero (1993, 1997), to name the strata above each one (**Figure 3**). This way, we separated the Honda Group in the Tatacoa Desert from bottom to top on the Cerro Gordo Beds, Chunchullo Beds (**Figure 5F**), Tatacoa Beds, Cerbatana Beds, La Venta Red Beds (**Figure 5A**), and El Cardon Red Beds. The Cerbatana Beds corresponds to the base of the Villavieja Formation and includes the Monkey Beds, Fish Beds and Ferruginous Beds. We kept the conglomerate as a separate unit (Cerbatana Conglomerate Beds, **Figures 5A,E**) as it is the most conspicuous unit in the region, which also extends laterally ~10 km, and marks the top of the La Victoria Formation (Guerrero, 1993, Guerrero, 1997). In naming the map units by the horizons at their bases, the unit at the base of the Honda Group would have been left unnamed. We therefore modified the original stratigraphic scheme by informally adding the San Alfonso Beds (**Figures 5B–D**) at the base of the La Victoria Formation to refer to those beds below the Cerro Gordo Beds

(horizon 1 of Guerrero (1993, 1997)), and directly above the mechanical basement (**Figure 3**). Additionally, we report the presence of strata seemingly older than the San Alfonso Beds. We additionally refined the mapped extent of younger alluvial deposits (**Figure 5G**).

The geologic map (**Figure 4**) defines a very gently folded, south- and southeast-dipping stratigraphic succession, resting in angular unconformity on Jurassic volcanoclastic basement of the Saldaña Formation (Cediel et al., 1981). This unconformity, defining the Natagaima Arch (Mojica and Franco, 1990; Schamel, 1991; Ramon and Rosero, 2006), beheads the hanging wall anticline of the east-verging Andalucia thrust fault (Villarroel et al., 1996). Erosion did not entirely remove the Cretaceous sequence near the easternmost edge of this hanging wall anticline. Here (quadrangle I7 in **Figures 4**, **6A**, **7** section A-A') the Albian Caballos Formation (**Figure 3**, sensu Florez and Carrillo, 1994) rests unconformably on the Saldaña Formation near the fault zone, which is marked by a sliver of black fossiliferous limestone less than 50 m across, probably part

FIGURE 7 | Cross-sections of the Tatacoa Desert. **(A–A')** Cross-section highlighting growth strata associated to the relatively small La Peralta and Cerro Gordo anticlines (quadrangle F3-G4 in **Figure 4**). Inset: field drawing of growth strata along the Arenosa creek ~ 2km to the southeast of the cross-section along the axis of the Cerro Gordo Anticline. **(B–B')** Cross-section showing the growth unconformity below the La Venta Red Beds inferred from the map (**Figure 4**) where strata in the northwestern flank of La Becerrera Anticline may also represent growth strata.

FIGURE 8 | Spatial attitude of bedding in the western flank of La Peralta Anticline showing three northwestern-dipping domains display progressively higher dips (quadrangle F3 in **Figure 4**). Field data (red dots) corroborates 3D model measurements (black dots). Inset shows render of steeply dipping strata.

of the Cenomanian–Turonian Villeta Group (**Figure 3**, Villamil and Arango, 1998). The footwall of this fault contains a sequence of northwest-dipping, massive mudstone and medium-grained sandstone, lithologically indistinguishable from strata typical of the La Victoria, and parts of the Villavieja formations (indeed mapped as such by Villarroel et al., 1996; Ingeominas, 2002). Crucially, the trace of the Andalucia Fault is fossilized by strata of the San Alfonso Beds, as these beds can be followed covering undisturbed the fault trace (**Figure 6A**). Lithic sandstone/mudstone strata in the footwall of the Andalucia Fault are therefore older than the oldest strata fossilizing the fault trace (San Alfonso Beds of La Victoria Formation) and left as an undifferentiated Miocene unit below the Honda Group (**Figure 6A**), perhaps correlative to the La Cira Formation (De Porta and De Porta, 1962).

The geologic map (**Figure 4**) also reveals two growth unconformities within strata of La Victoria Formation. In the northern third of the mapping area, strata of the Chunchullo and Tatacoa Beds are folded in two en-echelon, left-stepping, west- and northwest-verging anticlines (Cerro Gordo and La

Peralta anticlines, Guerrero (1993, 1997). Dips and thickness of strata define a fan-like pattern on the northwestern flanks of these folds (**Figure 7**, inset), with thickening strata dipping much more steeply near the axis of the anticline, suddenly thinning and flattening to regain low dips less than 250 m westwards (**Figure 8**). Satellite imagery and the geologic map (**Figure 6B**) show the truncations of strata near the southern tip of the Cerro Gordo anticline, diagnostic of growth unconformities. Another, larger growth unconformity is suggested by the contrasting structural attitude of strata towards the southeastern edge of the mapping area (**Figure 7**, section B–B'). Here, strata of the San Alfonso Beds are folded in an upright, tight NNE-trending, asymmetrical anticline (La Becerrera Anticline, Guerrero (1993, 1997). The Cerbatana, Tatacoa and Chunchullo Beds are thick, and well developed in the western flank of the anticline, but they are missing or severely thinned on the eastern flank (**Figure 4**, quadrangles H12 to I10).

The geologic map (**Figure 4**) also shows a deeply dissected, unconsolidated deposit with well-rounded, quartzite cobble and
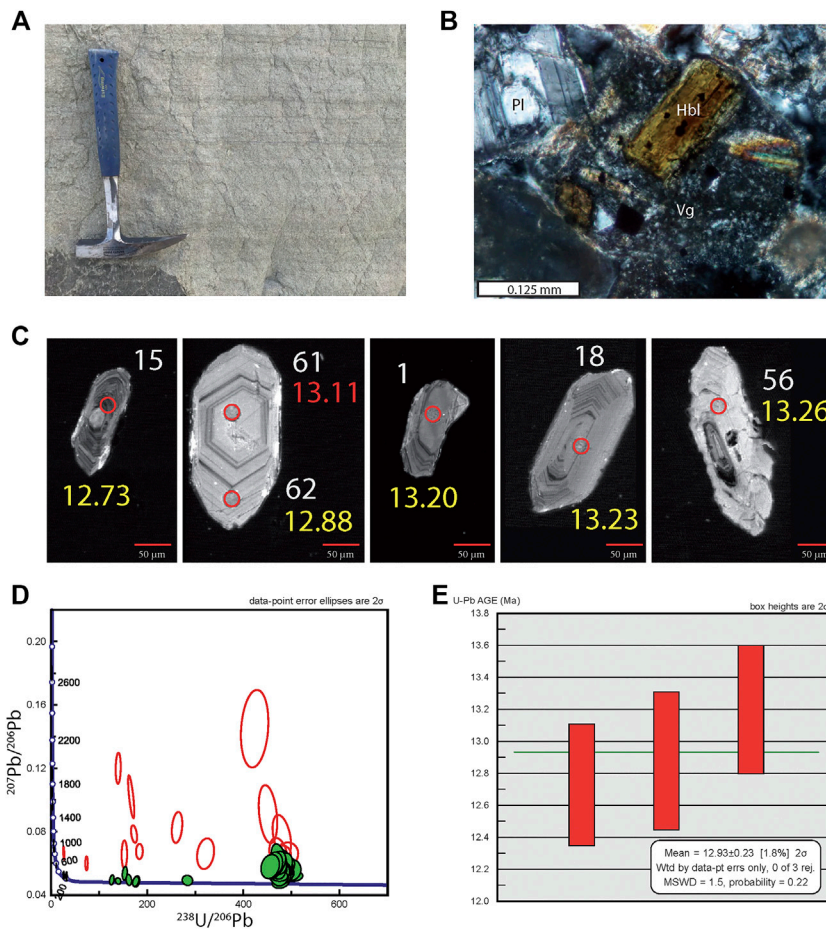
FIGURE 9 | Sample SEL-02 (coordinates: 3.27419 N, 75.1965 W). (A) Sampled strata in a plane parallel-bedded volcanoclastic unit near the top of the Tatacoa Beds (Figure 3). (B) Photomicrograph showing fresh detrital components, plagioclase (PL), hornblende (Hbl), surrounded by volcanic glass (Vg). C) Cathodo-luminescence of the five youngest zircons, note youngest ages in overgrowths (number in yellow: best age, number in red: discordant age). See SM2 for all images. (D) Tera–Wasserburg concordia diagram showing concordant (green, n = 47) and discordant (red, n = 15) U-Pb ages. (E) Detrital zircon maximum depositional age (MDA) calculated using weighted average of the youngest three U-Pb ages (Y3Z method of Coutts et al., 2019).

boulder clasts, within a characteristically red, muddy/sandy matrix (Figure 5G). This is typically preserved at hilltops, making them conspicuously flat, with steep, reddish edges (Figure 5G). The quartzite cobbles and pebbles, more resistant to erosion, act as a carapace protecting the sequence below from erosion, so these alluvial remains usually occupy the highest areas throughout the Tatacoa Desert. Differential removal of the finer-grained matrix of the coarse-grained deposit leaves behind reddish, cobble and pebble float that still protects the underlying strata from erosion, usually along the slopes of flat-topped hills. Remains of this unconsolidated deposit, and leftover float cobbles are ubiquitous. A thin, fine-grained unconsolidated deposit was also discriminated in the geologic map, and although much less prominent, it can be seen as flat terrain on top of dipping strata. It is unclear what is its relationship to the coarse-grained unconsolidated deposit, but being finer-grained, and located in lower topographic positions, it should be younger than the coarse-grained deposit. Near the eastern edge of the map, the coarse-grained deposit is found tilted to the east (Figure 4, quadrangle I10).

Geochronology

We actively sought volcanic ash beds interbedded within the sequence to place tighter constraints on depositional ages. Having found none, we settled for clastic beds nearly 30 m below the base of the Cerbatana Conglomerate Beds that contained the most volcanic components to extract detrital zircon grains and perform U-Pb LA-ICP-MS geochronology. We chose sample SEL-02 from a sandstone bed in banks of internally massive to plane-parallel bedded, laterally continuous beds, composed of fine-to medium-grained lithic arkose (quartz = 25%; feldspar = 47%; lithics = 28%) with flat lamination, and horizontal stratification structures at top and bottom, massive in between (Figure 9A). Sand-size fragments include non-altered angular clasts of plagioclase, K-feldspar, and hornblende with trace amounts of silt-size matrix (Figure 9B). Below this bed, the sequence shows a more typical La Victoria Formation sedimentary pattern characterized by fine-grained grey lithic sandstones interlayered with pinkish mudstones. Anderson et al. (2016) identified a similar lithic arkose in a sandstone unit also below

the Cerbanata Conglomerate Beds (their sample S5), and we recognized similar lithofacies in other localities in roughly the same stratigraphic position.

In our sample SEL-2 we performed 62 U-Pb, LA-ICPMS measurements on 61 zircon grains (**Figure 9C**). Fifteen of those measurements were rejected because they yielded high discordance or a large error age percentage (**Figure 9D**). Miocene ages are recorded in 24 grains (51%), where 23 grains (49%) yield ages younger than 20 Ma. The youngest age obtained in this analysis is 12.7 ± 0.38 Ma (see SM-2). All zircon grains younger than 14 Ma show elongated morphologies, while the youngest grain is fully prismatic (grain 62 in **Figure 9C**). Because we are seeking to constrain depositional ages, we use the three youngest zircons, including the external rim of grain 62, or 12.93 ± 0.23 Ma (**Figure 9E**, MSWD: 1.5).

DISCUSSION

The updated geologic map of the Tatacoa Desert (**Figure 4**) and additional geochronological work (**Figure 9**) help refine the Miocene drainages and paleogeography of this crucial paleontological locality. In the following paragraphs we document that active deformation was taking place during accumulation of strata of the La Victoria Formation, with the resulting growth unconformities. We then review new and existing detrital zircon geochronology in light of the updated geologic map, and suggest that the river system that transported the sediments of the Honda Group was sourced in active volcanic centers in today's Cauca Valley and the eastern flank of the Western Cordillera, draining eastward to the Amazon lowlands. We then use published data to document the time at which this Andean portal was closed.

Growth Strata

The northeast-trending, northwest-verging, fault-related Cerro Gordo and La Peralta anticlines were growing at the time of accumulation of the San Alfonso and Cerro Gordo Beds. These folds display a classic fan-like, cross-sectional geometry in their northwestern flanks (**Figures 6B,7** inset, **8**), typical of growth strata (e.g., Suppe et al., 1997). These relatively minor structures (only ~5 km long), caused strata of the Chunchullo and Cerro Gordo Beds to be thicker in their northwestern flanks, and thin, or pinch out entirely in their southeastern flanks (**Figure 7**). A growth unconformity is well developed near the southwestern tip of the Cerro Gordo Anticline, where steeply-dipping strata within the Chunchullo beds are truncated by gently-dipping strata to the northwest (**Figure 6B**, quadrangle E6 in **Figure 4**). Geochronological data indicates that these strata were accumulated between ~13.3 and 13.7 Ma (Flynn et al., 1997), and therefore date deformation and propagation of structures to this time interval (**Figure 4**).

A larger, and more significant unconformity developed as the NNE-trending La Becerrera Anticline grew. The Chunchullo, Tatacoa and Cerbatana Beds are well developed in its northwestern flank, but thin, or absent in its southeastern

flank (**Figure 7**, section B–B'). By analogy to the smaller structures described above, this anticline grew at the time of deposition of the Chunchullo, Tatacoa and Cerbatana Beds, served as the eastern limit for their extent, and only tighten after the accumulation of the La Venta Red Beds, which overlaps it. This growth unconformity therefore documents the propagation of deformation to between ~12.2 and 13.3 Ma (Flynn et al., 1997).

Geochronological Constraints

The updated geologic map (**Figure 4**) helps re-evaluate published geochronological data points (**Figure 3**). Consistent with its stratigraphic position, the lowest sample is also the oldest maximum depositional age in the sequence, in the San Alfonso Beds (sample Z1 14.4 ± 1.9 Ma, U-Pb, Anderson et al., 2016), albeit with a low fraction of zircons younger than 20 Ma (only 8%), and an analytical error large enough to overlap all other age determinations. Sample JG-R90-3 was also re-located to the lowest unit of La Victoria Formation (San Alfonso Beds) yielding the second oldest age within the sequence (13.778 ± 0.081 Ma, Ar/Ar in biotite, Flynn et al., 1997). In ascending stratigraphic order, Ar/Ar samples JG-R89-1 (13.651 ± 0.107 Ma) and JG R89-3 (13.767 ± 0.052 Ma) with overlapping analytical errors (Flynn et al., 1997), were both re-located near the top of the Cerro Gordo Beds, and suggest rapid accumulation rates. Sample JG-R90-1 (13.342 ± 0.408 Ma, Ar/Ar in hornblende, Flynn et al., 1997) in the upper part of the Chunchullo Beds shows maximum depositional ages (**Figure 3**) younger than detrital zircon samples Z2 and Z3 at the base of the overlying Tatacoa Beds with U-Pb age of 13.75 Ma (±0.9 and 0.4 Ma, respectively, Anderson et al., 2016). However, samples Z2 and Z3, besides having large analytical errors, plot stratigraphically above in the geologic map (**Figure 4**), and must therefore rework older volcanic units, and should not be taken as near-depositional ages. Further up stratigraphically, near the top of Cardon Red Beds, sample JG-R88-2 yielded a 12.21 ± 0.107 Ma (Ar/Ar in hornblende, Flynn et al., 1997), being the youngest age of the Villavieja Formation. While this sample plots in recent alluvial deposits (**Figure 4**), it was more likely collected in strata exposed along spotty outcrops along a creek bed. Other U-Pb detrital zircon samples with older detrital ages, and low fractions of young (less than 20 Ma) detrital populations (Z4 = 27%; Z5 to Z9 = 0–9%, Anderson et al., 2016), are most likely reworking older volcanic deposits and provide maximum accumulation ages far removed from a true depositional age.

Our U-Pb detrital zircon sample SEL-02 (12.93 ± 0.23 Ma, MSWD: 1.5, **Figure 9E**), collected in strata just 30 m below the base of the Cerbatana Conglomerate Beds is consistent with sample JG-R89-2 (12.512 ± 0.102 Ma in plagioclase and hornblende, Flynn et al., 1997), collected just above it (**Figure 3**). Both of these ages bracket the age of the conglomerate, and suggest fast accumulation rates (between 0.75 and 0.086 Ma), as suggested by Flynn et al. (1997), to explain the slightly discordant age of sample JG-R89-2 (**Figure 3**) with respect to the magnetostratigraphic data.

We interpreted the volcanic-rich bed where sample SEL-02 was collected, as the record of a diluted lahar deposit which may

FIGURE 10 | Huila Volcano, a massive ~5,600 m a.s.l. active composite volcano as seen from the Tatacoa Desert, looking west (see **Figure 1** for location). Eastward migration of a Miocene magmatic arc built these volcanic edifices (**Figure 1**) starting at ~4 Ma (Barberi et al., 1988; Ujueta, 1999; Torres-Hernandez, 2010), that along with contractional deformation along the flanks of the Central and Eastern cordilleras (Alfonso et al., 1994; Saeid et al., 2017), severed any fluvial communication between the Cauca and Magdalena valleys. Ridges in the foreground correspond to Oligocene molasse deposits involved in the east-vergent, fold-and-thrust belt at the toe of the Central Cordillera.

be the response of a major change in the hydraulic regime in the basin. The presence of almost fresh volcanic fragments, plagioclase, and hornblende (**Figure 9B**) suggests a short lag time between crystallization, exhumation erosion and deposition (e.g. Cawood et al., 2012), and requires volcanic sources located near the Tatacoa Desert (less than ~200 km, Johnsson et al., 1991; Amorocho et al., 2011).

Volcanic activity in the age range of the Honda Group strata (~12–14 Ma) is restricted in the Northern Andes to a northward-propagating, post-collisional magmatic arc that lit up as Nazca lithosphere subducted behind the accreted Panama arc. This magmatic arc extended from about 3°S (Bineli-Betsi et al., 2017), up to ~7°N along an axis located west of today's Central Cordillera (Wagner et al., 2017). The Upper Cauca–Patia magmatic center is part of this arc, with crystallization ages between 17 and 9 Ma (Leal-Mejia, 2011; Echeverri et al., 2015; Leal-Mejia et al., 2019). This magmatic center is located ~130 km to the west of the Tatacoa Desert (**Figure 1**), making it the only candidate for unstable volcanic fragments (e.g. hornblende, **Figure 9B**) to arrive unweathered (Johnsson et al., 1991; Amorocho et al., 2011) to the depositional basin of the Tatacoa Desert. This possible source however, is today located west of the axis of the Central Cordillera (**Figure 10**).

Paleogeography

Fossil fish fragments found in Honda Group strata firmly establish a middle Miocene connection between the fluvial systems of the Magdalena and Amazon basins before the rise of the southernmost Eastern Cordillera (Lundberg, 1997; Lundberg et al., 1998; Ballen and Moreno-Bernal, 2019). Paleocurrents measured in the Honda Group strata indicate an east-southeastward directed paleoflow (Guerrero, 1993; Guerrero, 1997; Anderson et al., 2016), resembling drainages in today's eastern Andean foothills (**Figure 1**). Detrital zircon geochronology in middle and late Miocene strata of both the southern Magdalena Valley and the Amazon Basin (**Figure 11**) is consistent with this paleogeographic configuration. Very similar middle Miocene, middle Eocene, and Jurassic detrital zircon age populations are found in Miocene strata of both basins (~11–12 Ma, Solimoes Formation, Kern et al., 2020).

Other sites with similar Miocene and Eocene detrital zircon populations include the middle to upper Miocene strata of the Amaga Formation (Montes et al., 2015), and the Cauca-Patia Basin (Echeverri et al., 2015). Both sites are located west of today's Central Cordillera (**Figure 1**), and both are derived from sources west of the Central Cordillera: 1) the Panama block (docked by ~15 Ma, Montes et al., 2015; Leon et al., 2018), as no other area of the Northern Andes contains such U-Pb zircon sources (Leal-Mejia, 2011; see discussion in; Jaramillo et al., 2017b; Leal-Mejia et al., 2019); and 2) the Miocene magmatic centers in the Cauca-Patia Basin (Echeverri et al., 2015; Wagner et al., 2017). Detrital zircon populations in the Tatacoa Desert and the Amazon Basin (**Figure 11**, and Fig. SM2) could have been sourced in the Cauca–Patia, and northwestern Andes, suggesting that these sites were once connected by the same fluvial system through today's Central and Eastern cordilleras.
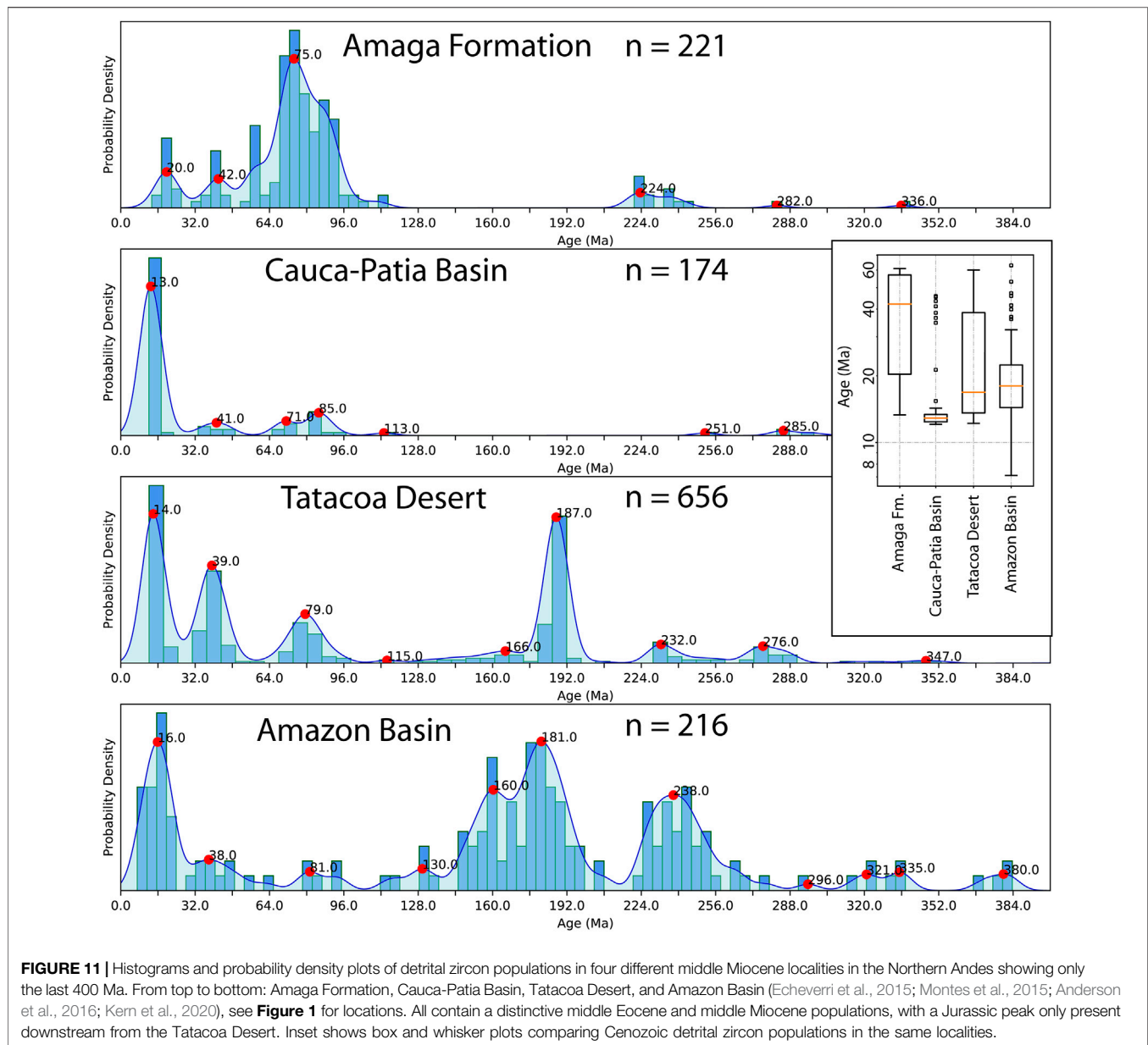
FIGURE 11 | Histograms and probability density plots of detrital zircon populations in four different middle Miocene localities in the Northern Andes showing only the last 400 Ma. From top to bottom: Amaga Formation, Cauca-Patia Basin, Tatacoa Desert, and Amazon Basin (Echeverri et al., 2015; Montes et al., 2015; Anderson et al., 2016; Kern et al., 2020), see **Figure 1** for locations. All contain a distinctive middle Eocene and middle Miocene populations, with a Jurassic peak only present downstream from the Tatacoa Desert. Inset shows box and whisker plots comparing Cenozoic detrital zircon populations in the same localities.

We therefore propose a paleogeographic interpretation where a river drained the docked Panama-Choco block, and the active volcanic centers in the Cauca Valley into the Tatacoa Desert, to reach the western Amazon Basin (**Figure 12**). This drainage would have not been impeded by either the Central or Eastern cordilleras at this time. Drainage connectivity across the Central Cordillera like the one we suggest here, is consistent with phylogeographic concordance factors of co-occurring groups of fresh water fish (*Hemibrycon*) between the Atrato-Darien (**Figure 1**) and southern Magdalena Valley drainages (Rincon-Sandoval et al., 2019). This lowland corridor would have therefore segmented the Andes at about 3°N, and further south (Cadena and Casado-Ferrer, 2019), in a fashion similar to a Marañon, or Western Andean Portal (Lundberg et al., 1998; Antonelli et al., 2009), during middle Miocene times.

The northernmost Central Andes, positive since at least latest Cretaceous times (Witt et al., 2017; Hurtado et al., 2018) would have defined the southern tip of this lowland portal (**Figure 2A**). Intense volcanic activity after ~4 Ma (Barberi et al., 1988; Van der Wiel, 1991; Ujueta, 1999; Torres-Hernandez, 2010) along the axis of the Real/Central Cordillera (**Figures 1,10**) resulted from flattening of the subducting Nazca slab (Wagner et al., 2017), and eastward migration of the Miocene magmatic arc. This Pliocene activity, and continued fault propagation (Alfonso et al., 1994; Saeid et al., 2017) built the final highland connection between the Central and Northern Andes, as well as between the Eastern and Central cordilleras (Ujueta, 1999), severing any connections to Amazonian drainages, and between the Cauca and Magdalena valleys (**Figure 1**).
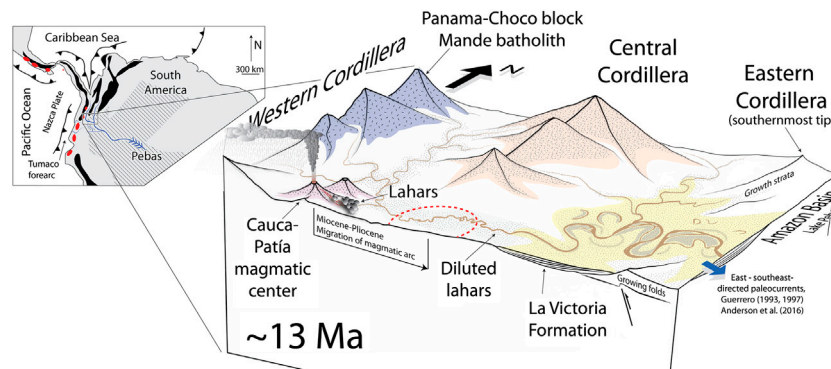
FIGURE 12 | Block-diagram illustrating a possible paleogeographic scenario for middle Miocene times (~13 Ma) in the Tatacoa Desert. Light yellow represent areas where subsidence and sediment accumulation took place. Dashed red line represents the future location of the Pliocene and younger magmatic arc of the Central Cordillera (**Figure 10**). Detrital geochronology (**Figure 11**), paleocurrent data (Guerrero, 1997; Anderson et al., 2016), and molecular fish data (Rincon-Sandoval et al., 2019) suggest connection of the volcanically active Cauca-Patia Basin (Leal-Mejia, 2011; Echeverri et al., 2015; Leal-Mejia et al., 2019), the recently accreted Panama-Choco block (Montes et al., 2015; Leon et al., 2018), with the Tatacoa Desert, itself connected to westernmost Amazonia's Pebas system. Dominant wind directions according to Sepulchre et al. (2009). Inset shows palinspastic reconstruction of the margin at the same time (Montes et al., 2019), showing significant relief in black (Montes et al., 2015; Witt et al., 2017), Pebas system extent and drainages in diagonal pattern (Lundberg and Chernoff, 1992; Wesselingh et al., 2001; Jaramillo et al., 2017a; Kern et al., 2020), and active magmatic centers in red (Echeverri et al., 2015; Bineli-Betsi et al., 2017; Wagner et al., 2017).

CONCLUSIONS

(1) Miocene strata preserved in the Tatacoa Desert contain the record of tectonic activity during the time that La Victoria and the base of Villavieja formations were accumulated ~12.2–13.7 Ma. NNE-trending anticlines (Cerro Gordo and La Peralta) grew at the time that the San Alfonso Beds and Cerro Gordo Beds (base of La Victoria Formation) accumulated. Similarly, the larger La Becerrera Anticline developed contemporaneously with the deposition of the Cerro Gordo Beds to Cerbatana Beds, generating significant growth unconformities.

(2) Possible sources for the detrital zircon grains (**Figure 11**) recovered in middle Miocene (Serravallian) strata of the Honda Group are located west today's Central Cordillera. This includes the Eocene magmatic rocks of the Panama-Choco block, and the middle Miocene magmatic rocks of the Cauca Valley (**Figure 12**). A matching detrital zircon signature (**Figure 11**) has been recovered from upper Miocene strata in the Amazon Basin to the east (Kern et al., 2020) suggesting that Amazon-like drainages may have operated since ~12 Ma.

(3) A Serravallian trans-Andean passage at ~3°N across the Central Cordillera (**Figure 11**) may have existed to allow both the Eocene and the Miocene detrital zircon populations to mix and accumulate in strata of the Tatacoa Desert. This lowland passage would have therefore communicated the late Pebas system (Wesselingh et al., 2001) in the western Amazonian Basin, to at least the Cauca Valley to the west (**Figure 12**).

(4) This Andean portal would have been open since at least 13–14 Ma, until a combination of fault propagation and intense volcanic activity during Pliocene times built the final connection joining the highlands of the Eastern and Central cordilleras.

DATA AVAILABILITY STATEMENT

The original contributions presented in the study are included in the article/**Supplementary Material**, further inquiries can be directed to the corresponding author.

AUTHOR CONTRIBUTIONS

Geologic mapping: CM, CS, RV, ES, FL, DM, LP-A, and JG. Geochronology: AB-T, ER, AvQ, AR-C; GIS: CM, SG and NH. Stratigraphy: GB, ER and AC. Geological background and writing of the paper: CM, GB, ES, AB and AC.

FUNDING

SUPPLEMENTARY MATERIAL

The Supplementary Material for this article can be found online at: https://www.frontiersin.org/articles/10.3389/feart.2020.587022/full#supplementary-material.

REFERENCES

Albert, J. S., Lovejoy, N. R., and Crampton, W. G. (2006). Miocene tectonism and the separation of cis-and trans-Andean river basins: evidence from Neotropical fishes. *J. South Am. Earth Sci.* 21 (1), 14–27.

Alfonso, C., Sacks, P., Secor, D., Rine, J., and Pérez, V. (1994). A Tertiary fold and thrust belt in the Valle del Cauca Basin, Colombian Andes. *J. South Am. Earth Sci.* 7 (3–4), 387–402.

Amezquita, F., and Montes, C. (1994). "Seccion geologica El Maco-Buenavista: estructura en el sector Occidental del Valle Superior del Magdalena," in *Estudios geologicos del Valle Superior del Magdalena: Bogota*. Editor F. Etayo-Serna (Bogotá:Universidad Nacional de Colombia-Ecopetrol), 601–636.

Amorocho, R., Bayona, G., and Reyes-Harker, A. (2011). Controles en la composición de arenas fluviales en la zona proximal de una cuenca de Antepais Tropical (Colombia). *Geol. Colomb.* 36, 163–178. doi:10.18257/raccefyn.632

Anderson, V. J., Horton, B. K., Saylor, J. E., Mora, A., Teson, E., Breecker, D. O., et al. (2016). Andean topographic growth and basement uplift in southern Colombia: implications for the evolution of the Magdalena, Orinoco, and Amazon river systems. *Geosphere*. 12 (4), 1–22. doi:10.1130/GES01294.1

Antonelli, A., Nylander, J. A., Persson, C., and Sanmartín, I. (2009). Tracing the impact of the Andean uplift on Neotropical plant evolution. *Proc. Natl. Acad. Sci. USA*. 106 (24), 9749–9754. doi:10.1073/pnas.0811421106

Ayala-Calvo, R., Bayona, G., Cardona, A., Ojeda, C., Montenegro, O., Montes, C., et al. (2012). The paleogene synorogenic succession in the northwestern Maracaibo block: tracking intraplate uplifts and changes in sediment delivery systems. *J. South Am. Earth Sci.* 39, 93–111. doi:10.1007%2F978-3-319-76132-9_7

Ballen, G. A., and Moreno-Bernal, J. W. (2019). New records of the enigmatic neotropical fossil fish *Acregoliath rancii* (Teleostei Incertae sedis) from the middle Miocene Honda group of Colombia. *Ameghiniana*. 56 (6), 431–440. doi:10.5710/AMGH.17.09.2019.3266

Bande, A., Horton, B. K., Ramírez, J. C., Mora, A., Parra, M., and Stockli, D. F. (2012). Clastic deposition, provenance, and sequence of Andean thrusting in the frontal Eastern Cordillera and Llanos foreland basin of Colombia. *Geol. Soc. Am. Bull.* 124 (1–2), 59–76. doi:10.1029/2011TC003089

Barberi, F., Coltelli, M., Ferrara, G., Innocenti, F., Navarro, J. M., and Santacroce, R. (1988). Plio-quaternary volcanism in Ecuador. *Geol. Mag.* 125 (1), 1–14.

Bayona, G. A., Montes, C., Cardona, A., Jaramillo, C., Ojeda, G., Valencia, V., et al. (2011). Intraplate subsidence and basin filling adjacent to an oceanic arc-continent collision: a case from the southern Caribbean-South America plate margin. *Basin Res.* 23, 403–422. doi:10.1111/j.1365-2117.2010.00495.x

Bayona, G., Baquero, M., Ramírez, C., Tabares, M., Salazar, A. M., Nova, G., et al. (2020). *Unravelling the widening of the earliest Andean northern orogen: Maastrichtian to early Eocene intra-basinal deformation in the northern Eastern Cordillera of Colombia: basin Research*.

Bayona, G., Cardona, A., Jaramillo, C., Mora, A., Montes, C., Caballero, V., et al. (2013). Onset of fault reactivation in the eastern Cordillera of Colombia and proximal Llanos basin; response to Caribbean south American convergence in early Palaeogene time. *Geol. Soc. Lond.* 377, 285–314.

Bayona, G., Cortes, M., Jaramillo, C., Ojeda, G., Aristizabal John, J., and Reyes-Harker, A. (2008). An integrated analysis of an orogen-sedimentary basin pair; latest Cretaceous-Cenozoic evolution of the linked Eastern Cordillera Orogen and the Llanos foreland basin of Colombia, *Geol. Soc. Am. Bull.* 120, 9–10. doi:10.1111/j.1365-2117.2009.00459.x

Bayona, G. (2018). El inicio de la emergencia de los Andes del norte: una perspectiva a partir del registro tectónico-sedimentológico del Coniaciano al Paleoceno. *Revista de la Academia Colombiana de Ciencias*. 42 (165), 364–378. doi:10.18257/raccefyn.632

Bineli-Betsi, T., Ponce, M., Chiaradia, M., Ulianov, A., and Camacho, A. (2017). Insights into the genesis of the epithermal Au-Ag mineralization at Rio Blanco in the Cordillera Occidental of southwestern Ecuador: constraints from U-Pb and Ar/Ar geochronology. *J. South Am. Earth Sci.* 80, 353–374. doi:10.1016/j.jsames.2017.10.004

Borrero, C., Pardo, A., Jaramillo, C. M., Osorio, J. A., Cardona, A., Flores, A., et al. (2012). Tectonostratigraphy of the Cenozoic Tumaco forearc basin (Colombian Pacific) and its relationship with the northern Andes orogenic build up. *J. South Am. Earth Sci.* 39, 75–92. doi:10.1007/s13202-019-0660-7

Caballero, V., Parra, M., Mora, A., Lopez, C., Rojas, L. E., and Quintero, I. (2013). Factors controlling selective abandonment and reactivation in thick-skin orogens: a case study in the Magdalena Valley, Colombia, *Geol. Soc. Lond.* 377, 343–367. doi:10.1144/SP377.4

Cadena, E.-A., and Casado-Ferrer, I. (2019). Late Miocene freshwater mussels from the intermontane Chota basin, northern ecuadorean Andes. *J. South Am. Earth Sci.* 89, 39–46. doi:10.1016/j.jsames.2018.10.012

Caicedo, J., and Roncancio, J. (1994). "El Grupo Gualanday como ejemplo de acumulacion sintectonica, en el Valle Superior del Magdalena, durante el Paleogeno," in *Estudios geologicos del Valle Superior del Magdalena*. Editor F. Etayo Serna (Bogota: Universidad Nacional de Colombia-Ecopetrol), 1001–1019.

Cande, S. C., and Kent, D. V. (1992). A new geomagnetic polarity time scale for the Late Cretaceous and Cenozoic. *J. Geophys. Res. Solid Earth*. 97 (B10), 13917–13951.

Cardona, A., Montes, C., Ayala, C., Bustamante, C., Hoyos, N., Montenegro, O., et al. (2012). From arc-continent collision to continuous convergence, clues from Paleogene conglomerates along the southern Caribbean-South America plate boundary. *Tectonophysics*. 580, 58–87. doi:10.1016/J.TECTO.2012.08.039

Cardona, A., Valencia, V., Bayona, G., Duque, J., Ducea, M., Gehrels, G., et al. (2011). Early subduction-€related orogeny in the northern Andes: Turonian to Eocene magmatic and provenance record in the Santa Marta Massif and Rancheria basin, northern Colombia. *Terra Nova*. 23 (1), 26–34. doi:10.1111/j.1365-3121.2010.00979.x

Cardona, A., Weber, M., Valencia, V., Bustamante, C., Montes, C., Cordani, U., et al. (2014). Geochronology and geochemistry of the Parashi granitoid, NE Colombia: tectonic implication of short-lived Early Eocene plutonism along the SE Caribbean margin. *J. South Am. Earth Sci.* 50, 75–92. doi:10.1590/2317-488920160030294

Carrillo, J. D., Forasiepi, A., Jaramillo, C., and Sánchez-Villagra, M. R. (2015). Neotropical mammal diversity and the Great American Biotic Interchange: spatial and temporal variation in South America's fossil record. *Front. Genet.* 5, 451. doi:10.3389/fgene.2014.00451

Cawood, P. A., Hawkesworth, C., and Dhuime, B. (2012). Detrital zircon record and tectonic setting. *Geology*. 40 (10), 875–878. doi:10.1130/G32945.1

Cediel, F., Mojica, J., and Macia, C. (1980). Definicion estratigrafica del Triasico en Colombia, Suramerica; formaciones Luisa, Payande y Saldana. Translated Title: stratigraphic definition of the Triassic in Colombia, South America; Luisa, Payande and Saldana formations. *Newsl. Stratigr*. 9 (2), 73–104. doi:10.1016/j.tecto.2004.12.024

Cediel, F., Mojica, J., and Macia, C. (1981). Las formaciones Luisa, Payandé y Saldaña sus columnas estratigráficas características. *Geol. Norandina*. 3 (1), 11–19.

Christophoul, F., Baby, P., and Davila, C. (2002). Stratigraphic responses to a major tectonic event in a foreland basin: the Ecuadorian Oriente Basin from Eocene to Oligocene times. *Tectonophysics*. 345 (1–4), 281–298. doi:10.1016/S0040-1951(01)00217-7

Compton, R. R. (1985). *Geology in the field*. New Jersey: John Wiley & Sons.

Cossio, U., Rodriguez, G., and Rodriguez, M. (1995). *Geología de la Plancha 283 Purificación: Inegominas, scale 1:100.000*.

Coutts, D. S., Matthews, W. A., and Hubbard, S. M. (2019). Assessment of widely used methods to derive depositional ages from detrital zircon populations. *Geosci. Front*. 10, 1421–1435. doi:10.1016/j.gsf.2018.11.002

De Porta, J., and De Porta, N. S. (1962). Discussion sobre las edades de las formaciones Hoyon, Gualanday y La Cira en la region de Honda-San Juan de Rioseco. *Boletin de geologia UIS*. 9 (1), 69–85.

Dickinson, W. R., and Gehrels, G. E. (2009). Use of U–Pb ages of detrital zircons to infer maximum depositional ages of strata: a test against a Colorado Plateau Mesozoic database. *Earth Planet Sci. Lett.* 288 (1), 115–125. doi:10.1016/j.gsf.2018.11.002

Dill, H. G., Buzatu, A., Balaban, S.-I., Ufer, K., Gomez, J., Birgaoanu, D., et al. (2020). The "badland trilogy" of the Desierto de la Tatacoa, upper Magdalena Valley, Colombia, a result of geodynamics and climate: with a review of badland landscapes. *Catena*. 194, 1–20.

Echeverri, S., Cardona, A., Pardo, A., Monsalve, G., Valencia, V. A., Borrero, C., et al. (2015). Regional provenance from southwestern Colombia fore-arc and intra-arc basins: implications for Middle to Late Miocene orogeny in the Northern Andes. *Terra Nova*. 27 (5), 1–8. doi:10.1111/ter.12167

Egüez, A., Gaona, M., and Albán, A. (2017). Mapa Geológico de la República del Ecuador, *Scale*. 21, 2881–2903. doi:10.1016/S0022-1694(02)00283-4

Etayo-Serna, F. (1994). "Epilogo; a modo de historia geológica del Cretacico en el valle superior del Magdalena," in *Estudios Geológicos del Valle Superior del Magdalena: Bogotá*. Editor F. Etayo-Serna (Bogotá: Universidad Nacional de Colombia), 1–4.

Florez, J. M., and Carrillo, G. A. (1994). "Estratigrafia de la sucesion litológica basal del Cretacico del valle superior del Magdalena," in *Estudios Geológicos del Valle Superior del Magdalena: Bogotá*. Editor F. Etayo-Serna (Bogotá: Universidad Nacional de Colombia), 1–26.

Flower, B. P., and Kennett, J. P. (1994). The middle Miocene climatic transition: east Antarctic ice sheet development, deep ocean circulation and global carbon cycling. *Palaeogeogr. Palaeoclimatol. Palaeoecol.* 108 (3-4), 537–555.

Flynn, J., Guerrero, J., and Swisher, C. (1997). "Geochronology of the Honda group," in *Vertebrate Paleontology in the Neotropics: the Miocene fauna of La Venta, Colombia*. Editors R. Kay, C. Madden, R. L. Cifelli, and J. Flynn (Washington, DC: Smithsonian Institution Press), 44–60.

Gomez, E., Jordan, T. E., Allmendinger, R. W., and Cardozo, N. (2005a). Development of the Colombian foreland-basin system as a consequence of diachronous exhumation of the northern Andes. *Geol. Soc. Am. Bull.* 117 (9), 1272–1292. doi:10.1306/06181411110.

Gomez, E., Jordan, T. E., Allmendinger, R. W., Hegarty, K., Kelley, S., and Heizler, M. (2003). Controls on architecture of the late Cretaceous to Cenozoic southern middle Magdalena valley basin, Colombia. *Geol. Soc. Am. Bull.* 115, 131–147. doi:10.1111/j.1365-3121.2010.00979.x

Gomez, E., Jordan, T. E., Allmendinger, R. W., Hegarty, K., and Kelley, S. (2005b). Syntectonic Cenozoic sedimentation in the northern middle Magdalena valley basin of Colombia and implications for exhumation of the northern Andes. *Geol. Soc. Am. Bull.* 117 (5-6), 547–569.

Grosse, E. (1926). *Estudio Geológico del Terciario Carbonífero de Antioquia en la parte Occidental de la Cordillera Central de Colombia entre el rio Arma y Sacaojal*. Berlin: Dietrich Reimer (Ernst Vohsen), 361.

Guerrero, J. (1993). *Magnetostratigraphy of the upper part of the Honda group and Neiva formation: miocene uplift of the Colombian Andes*. Durham: Duke University.

Guerrero, J., Sarmiento, G., and Navarrete, R. E. (2000). The stratigraphy of the W side of the Cretaceous Colombian Basin in the Upper Magdalena Valley. Reevaluation of selected areas and type localities including Aipe. *Guaduas, Ortega, and Piedras: Geol. Colomb.* 25, 45–110.

Guerrero, J. (1997). "Stratigraphy, sedimentary environments, and the Miocene uplift of the Colombian Andes," in *Vertebrate Paleontology in the Neotropics: the Miocene fauna of La Venta, Colombia*. Editors R. Kay, R. Madden, R. Cifelli, and J. Flynn (Washington DC: Smithsonian Institution Press), 15–43.

Guillong, M., vonvon Quadt, A., Sakata, S., Peytcheva, I., and Bachmann, O. (2014). LA-ICP-MS Pb–U dating of young zircons from the Kos–Nisyros volcanic centre, SE Aegean arc. *J. Anal. Atom. Spectrom.* 29 (6), 963–970. doi:10.1016/j.dib.2018.03.100

Haffer, J. (1967). Speciation in Colombian forest birds west of the Andes. *Am. Mus. Novit.* 2294, 1–57.

Hermelin, M. (2016). *Geomorphological landscapes and Landforms of Colombia, landscapes and Landforms of Colombia*. New York, NY: Springer, 1–21.

Herrera, F., Manchester, S., and Jaramillo, C. (2012). Permineralized fruits from the late Eocene of Panama give clues of the composition of forests established early in the uplift of Central America. *Rev. Paleobot. Palynol.* 175, 10–24. doi:10.1016/j.revpalbo.2012.02.007

Hilgen, F., Lourens, L., and van Dam, J. A. (2012). "The neogene period.," in *The geologic time scale 2012*. Editors F. M. Gradstein, J. G. Ogg, M. Schmitz, and G. Ogg (Netherlands: Elsevier), 923–978.

Hoorn, C., Wesselingh, F., Ter Steege, H., Bermudez, M., Mora, A., Sevink, J., et al. (2010). Amazonia through time: Andean uplift, climate change, landscape evolution, and biodiversity. *Science*. 330, 927–931. doi:10.1126/science.1194585

Hoorn, C., Guerrero, J., Sarmiento Gustavo, A., and Lorente Maria, A. (1995). Andean tectonics as a cause for changing drainage patterns in Miocene northern South America. *Geology Boulder*. 23 (3), 237–240.

Horton, B. K., Anderson, V. J., Caballero, V., Saylor, J. E., Nie, J., Parra, M., et al. (2015). Application of detrital zircon U-Pb geochronology to surface and subsurface correlations of provenance, paleodrainage, and tectonics of the Middle Magdalena Valley Basin of Colombia. *Geosphere*. 11 (6), 1790–1811. doi:10.1130/GES01251.1

Horton, B. K. (2018). Sedimentary record of Andean mountain building. *Earth Sci. Rev.* 178, 279–309. doi:10.3389/feart.2019.00353

Hurtado, C., Roddaz, M., Santos, R. V., Baby, P., Antoine, P.-O., and Dantas, E. L. (2018). Cretaceous-early Paleocene drainage shift of Amazonian rivers driven by Equatorial Atlantic Ocean opening and Andean uplift as deduced from the provenance of northern Peruvian sedimentary rocks (Huallaga basin). *Gondwana Res.* 63, 152–168. doi:10.1590/1982-0224-20180033

Ingeominas (2002). *Geologia de la plancha 303, Colombia, 1:100.000.Ingeominas, scale*.

Jaimes, E., and de Freitas, M. (2006). An Albian–Cenomanian unconformity in the northern Andes: evidence and tectonic significance. *J. South Am. Earth Sci.* 21 (4), 466–492. doi:10.1016/j.jsames.2006.07.011

Jaramillo, C., Romero, I., D'Apolito, C., Bayona, G., Duarte, E., Louwye, S., et al. (2017a). Miocene flooding events of western Amazonia. *Sci Adv.* 3 (5), e1601693. doi:10.1126/sciadv.1601693

Jaramillo, C. A., Montes, C., Cardona, A., Silvestro, D., Antonelli, A., and Bacon, C. D. (2017b). Conclusions by O'Dea et al. regarding formation of the Isthmus of Panama are not supported. *Sci. Adv.* 3 (6), e1602321. doi:10.1126/sciadv.1602321

Johnsson, M. J., Stallard, R. F., and Lundberg, N. (1991). Controls on the composition of fluvial sands from a tropical weathering environment: sands of the Orinoco River drainage basin, Venezuela and Colombia. *Geol. Soc. Am. Bull.* 103, 1622–1647.

Kay, R. F., Madden, R. H., Cifelli, R. L., and Flynn, J. J. (1997). *Vertebrate paleontology in the neotropics: the Miocene fauna of La Venta*. (Washington, Colombia: Smithsonian Institution Press).

Kern, A. K., Gross, M., Galeazzi, C. P., Pupim, F. N., Sawakuchi, A. O., Almeida, R. P., et al. (2020). Re-investigating Miocene age control and paleoenvironmental reconstructions in western Amazonia (northwestern Solimões Basin, Brazil). *Palaeogeogr. Palaeoclimatol. Palaeoecol.* 545, 109652. doi:10.1016/j.palaeo.2020.109652

Kolarsky, R. A., Mann, P., and Monechi, S. (1995). "Stratigraphic development of southwestern Panama as determined from integration of marine seismic data and onshore geology," in *Geologic and Tectonic Development of the Caribbean Plate boundary in southern Central America*. Editor P. Mann (Boulder, Colorado: Geological Society of America), Volume 295, 159–200.

Lamus, F., Bayona, G., Cardona, A., and Mora, A. (2013). Procedencia de las unidades Cenozoicas del sinclinal de Guaduas: Implicación en la evolución tectónica del sur del valle medio del Magdalena y orógenos adyacentes. *Bol. Geol.* 35, 1. doi:10.1016/j.earscirev.2019.102903

Leal-Mejia, H. (2011). *Phanerozoic gold metallogeny in the Colombian Andes: a tectono-magmatic approach*. Ph.D.: Universitat de Barcelona, 989.

Leal-Mejia, H., Shaw, R. P., and Melgarejo i Draper, J. C. (2019). "Spatial-Temporal migration of granitoid magmatism and the Phanerozoic Tectono-magmatic evolution of the Colombian Andes," in *Geology and tectonics of northwestern South America: the Pacific-Caribbean-Andean Junction: Cham*. Editors F. Cediel and R. P. Shaw (Springer International Publishing), 253–410.

Leon, S., Cardona, A., Parra, M., Jaramillo, J. S., Valencia, V., Chew, D., et al. (2018). Transition from collision to subduction: an example from Panama-Nazca Neogene interactions. *Tectonics*. 37, 1–21. doi:10.1002/2017TC004785

Ludwig, K. (2012). *User's manual for Isoplot 3.75—a geochronology toolkit for Microsoft Excel.*, Berkeley Geochronology Center Special Publication, 5, 75.

Lundberg, J. (1997). "Freshwater fishes and their paleobiotic implications," in *Vertebrate Paleontology in the Neotropics: the Miocene fauna of La Venta*. Editors R. Kay, R. Madden, R. Cifelli, and J. Flynn (ColombiaWashington: Smithsonian Isntitution), 67–91.

Lundberg, J. G., and Chernoff, B. (1992). *A miocene fossil of the Amazonian fish Arapaima (Teleostei, Arapaimidae) from the Magdalena River region of Colombia—Biogeographic and evolutionary Implications: Biotropica.*, 2–14.

Lundberg, J. G., Marshall, L. G., Guerrero, J., Horton, B., and Malabarba, M. (1998). *The stage for Neotropical fish diversification: a history of tropical South American rivers*.

Manco-Garces, A., Marin-Ceron, M. I., Sanchez-Plazas, C. J., Escobar-Arenas, L. C., Beltran-Triviño, A., and Von Quadt, A. (2020). Provenance of the Cienaga de Oro formation: unveiling the tectonic evolution of the Colombian Caribbean

margin during the Oligocene-early Miocene. *Bol. Geol.* 42 (3), 205–226. doi:10. 18273/revbol.v42n3-2020009

Mange, M. A., and Maurer, H. (1991). *Heavy minerals in Colour*. New York, NY: Springer.

Martin-Gombojav, N., and Winkler, W. (2008). Recycling of Proterozoic crust in the Andean Amazon foreland of Ecuador: implications for orogenic development of the northern Andes. *Terra Nova.* 20 (1), 22–31. doi:10. 1111/j.1365-3121.2007.00782.x

Miller, M. J., Bermingham, E., Klicka, J., Escalante, P., do Amaral, F. S., Weir, J. T., et al. (2008). Out of Amazonia again and again: episodic crossing of the Andes promotes diversification in a lowland forest flycatcher. *Proc. Biol. Sci.* 275 (1639), 1133–1142. doi:10.1098/rspb.2008.0015

Mojica, J., and Franco, R. (1990). Estructura y evolución tectónica del valle medio y superior del Magdalena, Colombia. *Geol. Colomb.* 17, 41–64.

Montes, C., Cardona, A., Jaramillo, C., Pardo, A., Silva, J., Valencia, V., et al. 2015). Middle Miocene closure of the Central American Seaway. *Science.* 348 (6231), 226–229. doi:10.1126/science.aaa2815

Montes, C., Bayona, G., Cardona, A., Buchs, D., Silva, C., Moron, S. E., et al. (2012). Arc-continent collision and orocline formation: closing of the Central American Seaway. *J. Geophys. Res.* 12, 156. doi:10.1029/2011JB008959

Montes, C., Restrepo-Pace Pedro, A., and Hatcher Robert, D., Jr. (2003). Three-dimensional structure and kinematics of the Piedras-Girardot fold belt; surface expression of transpressional deformation in the Northern Andes, *AAPG Memoir.* 79, 849–873.

Montes, C., Rodriguez-Corcho, A. F., Bayona, G., Hoyos, N., Zapata, S., and Cardona, A. (2019). Continental margin response to multiple arc-continent collisions: the northern Andes-Caribbean margin. *Earth Sci. Rev.* 198, 102903. doi:10.1016/j.earscirev.2019.102903

Mora, A., Parra, M., Strecker, M. R., Kammer, A., Dimate, C., and Rodriguez, F. (2006). Cenozoic contractional reactivation of Mesozoic extensional structures in the Eastern Cordillera of Colombia. *Tectonics.* 25, 20. doi:10.1029/2005TC001854

Mora, A., Reyes-Harker, A., Rodriguez, G., Teson, E., Ramirez-Arias, J. C., Parra, M., et al. (2013). *Inversion tectonics under increasing rates of shortening and sedimentation: Cenozoic example from the Eastern Cordillera of Colombia.* Geological Society, London, Special Publications, 377.

Moreno, F., Hendy, A., Quiroz, L., Hoyos, N., Jones, D., Zapata, V., et al. (2015). Revised stratigraphy of neogene strata in the Cocinetas basin, La Guajira, Colombia. *Swiss J. Palaeontol.* 28, 1–39. doi:10.1007/s13358-015-0071-4

Moreno-Sanchez, M., and Pardo-Trujillo, A. (2003). "Stratigraphical and sedimentological constraints on western Colombia: implications on the evolution of the Caribbean plate," *He Circum-Gulf of Mexico and the Caribbean: hydrocarbon habitats, basin formation, and plate tectonics.* Editors C. Bartolini, R. Buffler, and J. Blickwede (AAPG), Volume Memoir 79, 891–924.

Nie, J., Horton, B. K., Mora, A., Saylor, J. E., Housh, T. B., Rubiano, J., et al. (2010). Tracking exhumation of Andean ranges bounding the middle Magdalena valley basin. *Colomb. Geol.* 38 (5), 451–454. doi:10.1130/G30775.1

Nie, J., Horton, B. K., Saylor, J. E., Mora, A. s., Mange, M., Garzione, C. N., et al. (2012). Integrated provenance analysis of a convergent retroarc foreland system: U/Pb ages, heavy minerals, Nd isotopes, and sandstone compositions of the Middle Magdalena Valley basin, northern Andes, Colombia. *Earth Sci. Rev.* 110 (1), 111–126. doi:10.1016/j.jsames.2016.06.003

Ochoa, D., Hoorn, C., Jaramillo, C., Bayona, G., Parra, M., and De la Parra, F. (2012). The final phase of tropical lowland conditions in the axial zone of the Eastern Cordillera of Colombia: evidence from three palynological records. *J. S. Am. Earth Sci.* 39, 157–169. doi:10.1029/JB086iB11p10753

Parnaud, F., Gou, Y., Pacual, J.-C., Capello, M. A., Truskowski, I., and Passalacqua, H. (1995). "Stratigraphic synthesis of western Venezuela," Editors A. J. Tankard, S. Suarez, and H. J. Welsink (Petroleoum Basins of South AmericaAAPG), 62, 681–698.

Pennington, W. D. (1981). Subduction of the eastern Panama basin and Seismotectonics of northwestern South America. *J. Geophys. Res.* 86 (B11), 10753–10770.

Ramon, J. C., and Rosero, A. (2006). Multiphase structural evolution of the western margin of the Girardot subbasin, Upper Magdalena Valley, Colombia. *J. S. Am. Earth Sci.* 21 (4), 493–509. doi:10.1016/j.jsames. 2006.07.012

Reyes-Harker, A., Ruiz-Valdivieso, C. F., Mora, A., Ramirez-Arias, J. C., Rodriguez, G., De La Parra, F., et al. (2015). Cenozoic paleogeography of the Andean foreland and retroarc hinterland of Colombia. *AAPG (Am. Assoc. Pet. Geol.) Bull.* 99 (8), 1407–1453. 10.1126/sciadv.1601693.

Rincon-Sandoval, M., Betancur-R, R., and Maldonado-Ocampo, J. A. (2019). Comparative phylogeography of trans-Andean freshwater fishes based on genome-wide nuclear and mitochondrial markers. *Mol. Ecol.* 28 (5), 1096–1115. doi:10.1111/mec.15036

Rodriguez, G., and Sierra, M. I. (2010). Las Sedimentitas de Tripogadi y las Brechas de Trigana: Un registro de Volcanismo de Arco, Corrientes de Turbidez y Levantamiento Rapido Eoceno en el noroccidente de Sur America, *Geol. Colomb.* 35, 74–86. doi:10.1016/j.earscirev.2019.102903

Ruiz, G., Seward, D., and Winkler, W. (2004). Detrital thermochronology a new perspective on hinterland tectonics, an example from the Andean Amazon Basin, Ecuador. *Basin Res.* 16 (3), 413–430. doi:10.1111/j.1365-2117.2004. 00239.x

Saeid, E., Bakioglu, K., Kellogg, J., Leier, A., Martinez, J., and Guerrero, E. (2017). Garzón Massif basement tectonics: structural control on evolution of petroleum systems in upper Magdalena and Putumayo basins, Colombia. *Mar. Petrol. Geol.* 88, 381–401. doi:10.1016/B978-0-12-816009-1.00006-X

Sarmiento-Rojas, L. F. (2018). "Cretaceous stratigraphy and Paleo-facies maps of northwestern South America," in *Geology and tectonics of northwestern South America: Medellin.* Editors F. Cediel and H. Shaw John, 673–747.

Schamel, S. (1991). "*Middle and upper Magdalena basins, Colombia.,*" *Active margin basins.* Editor K. T. Biddle (Tulsa, OK: AAPG), 52, 283–301.

Sepulchre, P., Sloan, L. C., Snyder, M., and Fiechter, J. (2009). Impacts of Andean uplift on the Humboldt Current system: a climate model sensitivity study. *Paleoceanography and Paleoclimatology.* 24 (4), 1–11. doi:10.1029/2008PA001668

Slade, R., and Moritz, C. (1998). Phylogeography of Bufo marinus from its natural and introduced ranges. *Proc. Biol. Sci.* 265, 769–777. doi:10.1098/rspb.1998.0359

Suppe, J., Sàbat, F., Munoz, J. A., Poblet, J., Roca, E., and Vergés, J. (1997). Bed-by-bed fold growth by kink-band migration: Sant Llorenç de Morunys, eastern Pyrenees. *J. Struct. Geol.* 19 (3–4), 443–461.

Tavani, S., Arbues, P., Snidero, M., Carrera, N., and Muñoz, J. (2011). Open Plot Project: an open-source toolkit for 3-D structural data analysis. *Solid Earth.* 2, 53–63. doi:10.5194/se-2-53-2011

Tera, F., and Wasserburg, G. (1972). U-Th-Pb systematics in three Apollo 14 basalts and the problem of initial Pb in lunar rocks. *Earth Planet Sci. Lett.* 14 (3), 281–304.

Torres-Hernandez, M. P. (2010). *Petrografía, geocronología y geoquímica de las ignimbritas de la formación Popayán, en el contexto del vulcanismo del suroccidente de Colombia [M.Sc. Universidad EAFIT].*, 132.

Ujueta, G. (1999). La Cordillera Oriental colombiana no se desprende de la Cordillera Central. *Geol. Colomb.* 24, 3–28.

Van der Hammen, T. (1958). Estratigrafía del Terciario y Maastrichtiano continentales y tectogénesis de los Andes colombianos. *Bol. Geol.* 6 (1–3), 1–56.

Van der Wiel, A. (1991). *Uplift and volcanism of the SE Colombian Andes in relation to Neogene sedimentation in the upper Magdalena valley [PhD. Agricultural University of Wageningen].*, 208.

Van der Wiel, A., and Van den Bergh, G. (1992). Uplift, subsidence, and volcanism in the southern Neiva basin, Colombia, Part 1: Influence on fluvial deposition in the Miocene Honda formation. *J. South Am. Earth Sci.* 5 (2), 153–173.

Villamil, T., and Arango, C. (1998). "Integrated stratigraphy of latest Cenomanian and early Turonian facies of Colombia," *Paleogeographic evolution and non-glacial Eustacy.* Editors L. Pindell James and L. Drake Charles (Tulsa, OK: Northern South AmericaSEPM), 58, 129–159.

Villamil, T. (1999). Campanian–Miocene tectonostratigraphy, depocenter evolution and basin development of Colombia and western Venezuela. *Palaeogeogr. Palaeoclimatol. Palaeoecol.* 153 (1), 239–275.

Villamil, T. (1998). "Chronology, relative sea-level history and a new sequence stratigraphic model for basinal Cretaceous facies of Colombia," in *Paleogeographic evolution and non-glacial Eustacy.* Editors L. Pindell James and L. Drake Charles (Tulsa, OK: Northern South AmericaSEPM), 58, 161–216.

Villarroel, C., Setoguchi, T., Brieva, J., and Macia, C. (1996). Geology of the La Tatacoa "desert" (Huila, Colombia): Precisions on the stratigraphy of the Honda group, the evolution of the" Pata high" and the presence of the La Venta fauna:

Memoirs of the Faculty of science. *Kyoto University, Series of Geology and Mineralogy*. 58, 41–66.

Von Quadt, A., Gallhofer, D., Guillong, M., Peytcheva, I., Waelle, M., and Sakata, S. (2014). U–Pb dating of CA/non-CA treated zircons obtained by LA-ICP-MS and CA-TIMS techniques: impact for their geological interpretation. *J. Anal. Atom. Spectrom*. 29 (9), 1618–1629. doi:10.1039/c4ja00102h

Wagner, L., Jaramillo, J., Ramirez-Hoyos, L., Monsalve, G., Cardona, A., and Becker, T. (2017). Transient slab flattening beneath Colombia. *Geophys. Res. Lett*. 44 (13), 6616–6623. doi:10.1002/2017GL073981

Weber, M., Cardona, A., Paniagua, F., Cordani, U., Sepúlveda, L., and Wilson, R. (2009a). The Cabo de la Vela Mafic-ultramafic Complex, northeastern Colombian Caribbean region: a record of multistage evolution of a late Cretaceous intra-oceanic arc. *Geol. Soc. Lond*. 328, 549–568.

Weber, M., Cardona, A., Wilson, R., Gomez, J., and Zapata, G. (2009b). High-pressure rocks from the Colombian Caribbean; record of a changing convergent margin. *Geochem. Cosmochim. Acta*. 71, A1095.

Weir, J. T., and Price, M. (2011). Andean uplift promotes lowland speciation through vicariance and dispersal in Dendrocincla woodcreepers. *Mol. Ecol*. 20 (21), 4550–4563. doi:10.1111/j.1365-294X.2011.05294.x

Wesselingh, F., Räsänen, M., Irion, G., Vonhof, H., Kaandorp, R., Renema, W., et al. (2001). Lake Pebas: a palaeoecological reconstruction of a Miocene, long-lived lake complex in western Amazonia. *Cainozoic Res*. 1 (1/2), 35–68. doi:10.1371/journal.pone.0199201

Witt, C., Rivadeneira, M., Poujol, M., Barba, D., Beida, D., Beseme, G., et al. (2017). Tracking ancient magmatism and Cenozoic topographic growth within the Northern Andes forearc: Constraints from detrital U-Pb zircon ages. *Bulletin*. 129 (3–4), 415–428. doi:10.1029/2019TC005967

Woodring, W. P. (1957). Geology and description of Tertiary mollusks (gastropods; trochidae to Turritellidae). Geology and paleontology of Canal Zone and adjoining parts of Panama. *U. S. Geol. Surv. Prof. Pap*. 306-A, 145.

Xie, X. Y., Mann, P., and Escalona, A. (2010). Regional provenance study of Eocene clastic sedimentary rocks within the South America-Caribbean plate boundary zone using detrital zircon geochronology. *Earth Planet Sci. Lett*. 291 (1–4), 159–171. doi:10.1086/668683

Zachos, J., Pagani, M., Sloan, L., Thomas, E., and Billups, K. (2001). Trends, rhythms, and aberrations in global climate 65 Ma to present. *Science*. 292 (5517), 686–693. doi:10.1126/science.1059412

Zapata, S., Cardona, A., Montes, C., Valencia, V., Vervoort, J., and Reiners, P. (2014). Provenance of the Eocene soebi blanco formation, Bonaire, Leeward Antilles: Correlations with post-Eocene tectonic evolution of northern South America. *J. South Am. Earth Sci*. 52, 179–193. doi:10.1007%2F978-3-319-55787-8_18